

**RHESUS RHADINOVIRUS ENCODES A FUNCTIONAL HOMOLOGUE OF
HUMAN CD200**

by

Carly L. Langlais

A DISSERTATION

Presented to the Department of Molecular Microbiology and Immunology
and the Oregon Health & Science University School of Medicine
in partial fulfillment of the requirements for the degree of
Doctor of Philosophy

December 2005

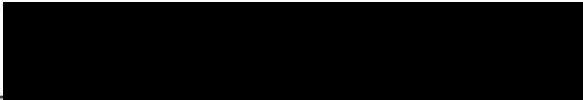
School of Medicine
Oregon Health & Science University


Certificate of Approval

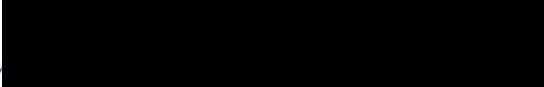
This is to certify that the Ph.D. dissertation of


Carly L. Langlais

has been approved


Scott Wong, Ph.D., *thesis advisor*


Ashlee Moses, Ph.D., *committee chair*


Mihail Jordanov, Ph.D., *committee member*


Mark Slifka, Ph.D., *committee member*


Deborah Lewinsohn, Ph.D., *committee member*

TABLE OF CONTENTS

List of figures and tables.....	p. v
Acknowledgements.....	p. vi-vii
Abstract.....	p. viii-ix

Chapter 1 – Introduction

1. Human herpesviruses

- a. Classification.....p. 1-2
- b. Structure.....p. 2-3
- c. General life cycle.....p. 3-9
- d. Human herpesvirus and disease.....p. 9-11
- e. Primary immune response to herpesvirus infection
 - i. General characteristics.....p. 11-14
 - ii. Human gammaherpesvirus specific immunity.....p. 14-16

2. Human herpesvirus 8 (HHV-8)/Kaposi's sarcoma-associated herpesvirus

(KSHV)

- a. Identification and classification of a Kaposi's sarcoma-associated herpesvirus.....p. 16-17
- b. HHV-8 associated diseases
 - i. Kaposi's sarcoma.....p. 17-20
 - ii. Primary effusion lymphoma.....p. 20-21
 - iii. Multicentric Castleman's disease.....p. 21

c.	Viral genes associated with pathogenesis.....	p. 24
d.	Models for studying HHV-8.....	p. 24-26
3.	Membrane proteins with immunoglobulin superfamily domains	
a.	Characteristics.....	p. 26-27
b.	Interactions.....	p. 27-28
4.	CD200	
a.	Characteristics.....	p. 28-31
b.	CD200-CD200R.....	p. 21-34
c.	Viral CD200 homologues.....	p. 34-37
5.	HHV-8 encoded viral CD200 homologue	
a.	Function.....	p. 38
b.	Transcription of HHV-8 K14.....	p. 38-39
c.	Implications for vCD200 expression during infection.....	p. 39-43
6.	Rhesus macaque rhadinovirus (RRV): a nonhuman primate model for HHV-8 infection	
a.	Identification and classification of RRV.....	p. 43-44
b.	RRV associated diseases.....	p. 44-45
c.	RRV ORFs associated with pathogenesis.....	p. 45
d.	RRV as a model for HHV-8 pathogenesis.....	p. 49

7. RRV vCD200 as a model for HHV-8 vCD200 pathogenesis

- a. Preliminary analysis of RRV R15.....p. 49-50
- b. Overview of thesis project.....p. 50-51
- c. Significance of this work.....p. 51-52
- d. Author's contributions.....p. 52

Chapter 2 – Manuscript #1

Splicing of rhesus rhadinovirus R15 and ORF74 bi-cistronic transcripts during lytic infection and analysis of effects on production of vCD200 and vGPCR.....p. 53-80

Chapter 3 – Manuscript #2

Rhesus rhadinovirus R15 encodes a functional homologue of human CD200.....p. 81-114

Chapter 4 – Summary and conclusions

1. Characterization of R15 transcripts during RRV infection

- a. Classification of R15 transcripts.....p. 115
- b. Unique splicing of R15 transcripts.....p. 115-116
- c. Protein expression from spliced transcripts.....p. 116-117

2. Assessing function of RRV vCD200	
a. Determining a suitable cell type for assessing RRV vCD200 function.....	p. 117-118
b. RRV vCD200-Fc.....	p. 118
c. Myeloid cell treatment with RRV vCD200-Fc.....	p. 118
3. Role of vCD200 during RRV infection	
a. Expression of R15 during RRV infection.....	p. 119-120
b. Model of RRV vCD200 action during infection.....	p. 120-121
4. Future directions.....	p. 124
5. Final conclusions.....	p. 124-125

Appendices

1. Assessing RRV vFLIP anti-apoptotic activity.....	p. 127-138
2. Transcriptional profile of RRV lytic infection.....	p. 139-149

<u>References</u>.....	p. 150-188
-------------------------------	-------------------

LIST OF FIGURES AND TABLES

<u>Figure</u>	<u>Page Number(s)</u>
1.1.....	4-5
1.2.....	22-23
1.3.....	29-30
1.4.....	35-36
1.5.....	40-41
1.6.....	46-47
1.7.....	48
2.1.....	73-74
2.2.....	75-76
2.3.....	77-78
2.4.....	79-80
3.1.....	106-107
3.2.....	108
3.3.....	109
3.4.....	110-111
3.5.....	112-113
3.6.....	114
4.1.....	122-123
A1.1.....	133-134
A1.2.....	135-136
A1.3.....	137-138

<u>Table</u>	<u>Page Number(s)</u>
1.1.....	33
A2.1.....	145
A2.2.....	146
A2.3.....	147-148
A2.4.....	149

ACKNOWLEDGEMENTS

While the production of the work contributing to this dissertation required many hours of experimentation and preparation, there is a larger component, a support system that has made all of this work possible. I would first like to thank my advisor, **Scott Wong** for his scientific ideas and support during my graduate career. The members of my thesis advisory committee, **Mihail Jordanov**, **Ashlee Moses**, and **Mark Slifka** have been most helpful in guiding my thesis projects, and keeping me on track. In addition, I would like to extend thanks to **Deborah Lewinsohn** for serving on my thesis exam committee.

In addition to academic support, I have been very fortunate to have a supportive family in all of the decisions involved in my life. Both of my parents, **Sharon Malloy** and **Lynn Pratt** have allowed me to develop goals and pursue my dreams, and I am grateful for their continual belief in my abilities. My two brothers, **Matthew Gray** and **Scott Gray**, have always looked out for me as their “little sister,” and have set great examples of achieving personal success that I strive to achieve myself.

Moving from Michigan, where I grew up and went to college, to Oregon by myself was comforted by great friends and fellow students. Discussions of ‘experiments gone bad,’ and studying sessions seemed to make the trials and tribulations of graduate school seem less trying. One particular friend of mine, **Ryan Estep**, has played an outstanding role in providing scientific advice and opinions, as well as in areas far from science.

The most influential person during my graduate studies was my husband, **Kristofor Langlais**. We met in graduate school and developed a friendship through

studying and rock climbing together. I have learned so much from Kris's positive outlook on life and from his ability to keep an eye on the larger picture that is life. Exploring Oregon's most beautiful wilderness and scenery together, we shared our ideas and thoughts, and learned from each other. It was Kris that was always there to celebrate small victories with me, encourage me, and inspire me to the finish line of graduation. I am forever grateful.

ABSTRACT

The most recently discovered human herpesvirus is the gammaherpesvirus, human herpesvirus-8 (HHV-8), also referred to as Kaposi's sarcoma-associated herpesvirus due to the etiological role of this virus in Kaposi sarcoma (KS) lesions. Within immunocompromised hosts, such as AIDS patients, HHV-8 is also associated with the development of B cell abnormalities including primary effusion lymphoma (PEL), and multicentric Castelman's disease (MCD). To understand viral mechanisms involved in the development of these malignancies, an animal model of HHV-8 infection is necessary. Rhesus rhadinovirus (RRV) is accepted as the rhesus macaque homologue of HHV-8, and has been promising for use as an animal model of HHV-8 infection within an immunocompromised host. Specifically, immunocompromised rhesus macaques infected with RRV develop lymphoproliferative disease resembling MCD in humans.

Potential viral open reading frames (ORFs) contributing to viral pathogenesis have been identified in RRV. These ORFs encode for proteins that promote angiogenesis and cellular survival, as well as those that work to evade the host immune system. One of the RRV ORFs of interest is R15, which encodes for a viral homologue of CD200 (vCD200). CD200 is a membrane glycoprotein that binds to its receptor (CD200R) on the surface of myeloid cells and some T cells, resulting in an anti-inflammatory response from these cells. In addition to RRV vCD200, other vCD200 homologues have been identified in HHV-8 (K14) and also in myxoma virus (M141R). Both of these viral proteins function similarly to CD200 in that they control activation of cells of myeloid lineage, shifting their cytokine profile toward a type 2, anti-inflammatory, response.

Here, RRV vCD200 is characterized. We demonstrate that the transcript encoding vCD200 is expressed at a late timepoint (72 hr.) during RRV lytic infection, and is bicistronic with ORF74, which encodes the transforming viral G protein-coupled receptor (vGPCR). In addition, we have identified a splicing event within the R15-ORF74 bicistronic transcript, in which 360 bp of sequence are removed. Interestingly, this spliced region of the R15-ORF74 transcript corresponds to the transmembrane domain of vCD200, allowing for a secreted version of vCD200 to be made from this transcript. This type of splicing event does not occur within the HHV-8 K14-ORF74 transcript.

Next, we sought to determine if RRV R15 encodes for a functional vCD200 homologue. For these studies, a soluble form of vCD200 was generated through the fusion of the predicted extracellular domain of vCD200 with the Fc fragment of human IgG₁.

Following incubation with vCD200-Fc, human monocyte-derived macrophages were demonstrated to produce reduced levels of the type 1 cytokine, tumor necrosis factor (TNF) at the RNA and protein levels in comparison to cells treated with Fc alone. Rhesus macaque monocyte-derived macrophages also responded to vCD200-Fc through secretion of reduced amounts of TNF. In addition a monoclonal antibody specific for RRV vCD200 revealed that this protein is expressed on the surface of rhesus fibroblasts during lytic infection. From these observations, we were able to conclude that RRV, like HHV-8 and myxoma virus, has successfully pirated a functional homologue of the immune regulator CD200.

Chapter 1

Introduction

1. Human herpesviruses

a. *Classification*

The *Herpesviridae* family is subdivided into three subfamilies based on cellular tropism, growth characteristics and host range (73). These three subfamilies are *Alphaherpesvirinae*, *Betaherpesvirinae*, and *Gammaherpesvirinae*. The subfamily *Alphaherpesvirinae* contains the genus *Simplexvirus* that includes the human pathogens human herpesviruses 1 and 2 (herpes simplex viruses 1 and 2). Also within the subfamily *Alphaherpesvirinae* is the genus *Varicellovirus*, which includes human herpesvirus 3 (varicella-zoster virus), pseudorabies virus, and equine herpesvirus 1 (74). Members of the *Alphaherpesvirinae* subfamily are similar in their variable host range and their short reproductive cycle. Infections with members of the *Alphaherpesvirinae* subfamily often result in host cell destruction, however, these viruses have the capacity to establish a latent infection primarily within sensory ganglia (73). The *Betaherpesvirinae* subfamily includes the genera *Cytomegalovirus* (human herpesvirus-5 [human cytomegalovirus]) and *Roseolovirus* (human herpesviruses-6 [A and B variants] and -7) (74). Viruses within the *Betaherpesvirinae* subfamily exhibit a restricted host range, a long reproductive cycle, and slow progression of infection in culture. Cells infected with viruses from this subfamily become enlarged (cytomegalia) and often proceed to a latent state of infection. Specifically, latent virus can be found residing in secretory glands, lymphoreticular

cells, kidneys, and other tissues of infected hosts (73). The third subfamily within the *Herpesviridae* family is *Gammaherpesvirinae*, which includes the genus *Lymphocryptovirus* (gamma-1) containing human herpesvirus-4 (Epstein-Barr virus). The genus *Rhadinovirus* (gamma-2) is also included in the *Gammaherpesvirinae* subfamily and includes herpesvirus saimiri and human herpesvirus-8/Kaposi's sarcoma-associated herpesvirus (74). Members of the *Gammaherpesvirinae* demonstrate restricted growth in either T or B lymphocytes, while some members of this subfamily are capable of undergoing lytic replication within epithelial, endothelial, or fibroblast cells (2, 73, 191). Like other herpesviruses, those within this subfamily enter a state of latency, however, latency is primarily observed within lymphoid tissue (73).

b. Structure

Despite differences in genomic sequence, herpesviruses share a common structural design. Herpesvirus virions are either spherical or pleomorphic with an overall diameter of 150-200 nanometers (nm). These virions consist of four components: an envelope, a tegument, a nucleocapsid, and a core (Figure 1.1). Beginning with the outermost structure, we will examine the components of the herpesvirus virion. The envelope comprises the outer covering of herpesvirus virions. Within the lipid bilayer of the envelope are spike-shaped surface glycoproteins that are important for interactions with and entry into host cells. This lipid bilayer is derived from the altered membranes of the host cell during viral egress (73, 74). The tegument of virions is made of amorphous protein material and surrounds the

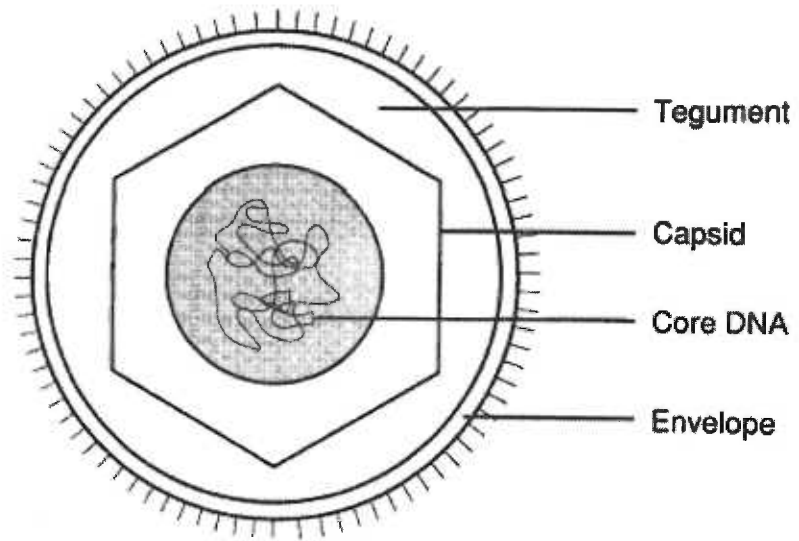
nucleocapsid. The icosahedral nucleocapsid of herpesvirus virions is $\sim 1,250$ Å in diameter and contains 162 capsomeres. All herpesvirus capsids examined to date possess a triangulation (T) number of 16, a feature unique to herpesviruses (216). Within the core resides the large linear, double-stranded DNA genome (~ 125 -250 kilobases [kb]), which is sometimes found wrapped around a toroid-shaped protein core (74, 216). Depending on virus subfamilies and genera, herpesvirus genomic sequences have differing arrangements. For example, the genome may contain two covalently linked components, the L (long) and S (short), while some herpesviruses contain only an L component to their genome. Repeat sequences (>100 base pair [bp]) are found at the ends and/or internally within the genomes, with locations and lengths of repeats varying depending on virus type (73). In addition, herpesvirus virions contain at least 30 structural proteins and a greater number of nonstructural proteins including DNA binding proteins, and those with enzymatic activity, including a DNA polymerase, a protease, and kinases (74).

c. General life cycle

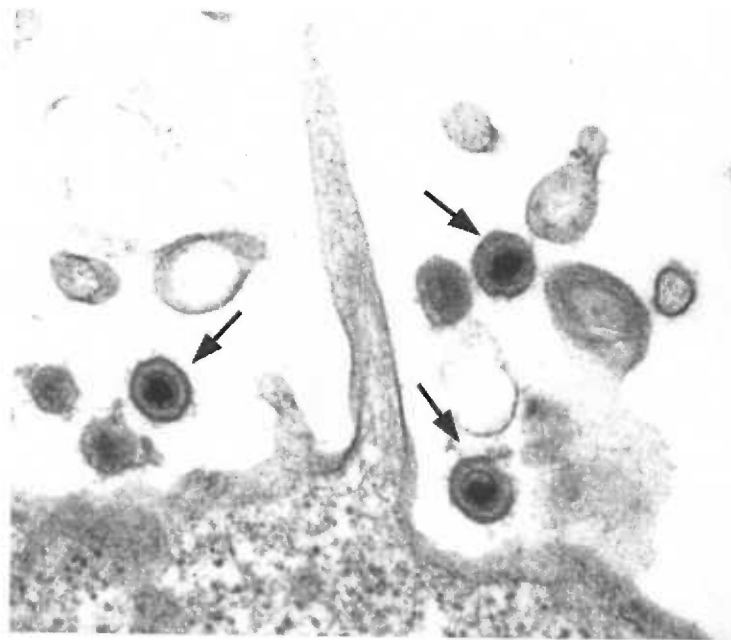
To initiate entry into the susceptible host cell, the herpesvirus engages specific receptor(s) on the host cell surface with viral glycoproteins in the lipid bilayer of the viral envelope. Many glycoproteins are likely involved in this process and three are believed to be essential for all herpesvirus entry: glycoprotein B (gB), gH, and gL. As these glycoproteins are required for entry, their sequences are highly conserved

Figure 1.1 (A) Diagram showing typical herpesvirus structure. *Figure adapted from (186).* (B) Morphology of HHV-8 virions produced from the KS-1 cell line. Arrows indicate fully mature virions. *Figure adapted from (2).*

A.



B.



among herpesviruses, with gB having highest sequence identity between herpesviruses. Most of the host range of herpesvirus infections can be explained by the nature of cell surface binding and the entry receptors encoded by the various herpesviruses (202).

Two types of receptors exist and play different roles during viral attachment and entry. The so-called “binding receptors” serve the purpose of concentrating viruses close to the cell surface, facilitating the events to follow. The second type of receptors are known as “entry receptors;” they allow for fusion to occur between the viral and host cell membranes during the entry process (202). Some viruses require endocytosis and acidification of the endosome during entry. gB, gH, and gL are key players in this fusion process for all herpesviruses, while some herpesviruses contain unique glycoproteins that likely allow for an enhanced host range, binding to a larger number of receptors on target cells. Examples of unique glycoproteins are gC and gD, which are conserved among neurotropic alphaherpesviruses and are absent from members of the betaherpesviruses and gammaherpesviruses (201). While many cellular receptors likely exist for herpesvirus entry, heparan sulfate is shared as a cellular receptor for HSV-1 and HHV-8 viral entry through binding of gB (4, 202).

Following the fusion event and shedding of the viral envelope, tegument proteins and the nucleocapsid are released into the permissive cell. Herpesvirus tegument proteins can aid in preparing the cell for optimal viral replication through employing various mechanisms. Specifically, tegument proteins have been demonstrated to modulate the cell cycle (110, 135), activate transcription of viral genes (17, 72, 115, 134, 234), and turn off host cell gene expression (193). In

addition, tegument proteins are believed to aid in targeting of the viral nucleocapsid to the nuclear pore where the viral DNA enters the host cell nucleoplasm (74). It is believed that the tegument proteins which remain attached to the viral nucleocapsid, such as VP1/2 and UL37 of alphaherpesviruses, aid in this transport and nuclear targeting of the nucleocapsids (138).

Once viral DNA is in the nucleus, viral transcription is initiated, following a tightly coordinated and regulated program of gene expression. While many viral factors play significant roles at all stages of infection, transcription of viral genes is dependent on the host RNA polymerase II (73). During lytic replication, the first set of three viral gene classes to be expressed is the immediate-early (or α) genes. A characteristic of immediate-early genes is that they are capable of being expressed in the absence of viral protein synthesis. Further, most proteins from this class of genes act as regulators of production of the second classes of viral genes, the early (or β) genes. The early genes require the expression of immediate-early genes, and most proteins arising from the early gene class are involved in viral nucleic acid metabolism. Following successful early gene expression, the late (or γ) genes are expressed (73). Products of the late genes are often structural components of the virus, which are necessary to generate infectious progeny virus particles.

Categorizing a viral gene to a particular class can be facilitated by the use of chemical metabolic inhibitors during *in vitro* viral infection. Specifically, inhibiting protein synthesis through the use of cycloheximide (CHX) identifies genes belonging to the immediate-early class. DNA replication can be blocked through the use of phosphonoacetic acid (PAA), allowing for the identification of early genes. Late

genes will be blocked by both CHX and PAA, therefore, genes of this kinetic class can be identified when these metabolic blocks are removed and later time points post-infection are examined, allowing for adequate expression of immediate-early and early genes.

With viral proteins made, virus assembly can proceed. Viral DNA is replicated via a rolling circle mechanism and packaged into preformed capsids within the nucleus (74, 144). These capsids must exit the nucleus to gain access to the extracellular environment and infect new host cells through a process termed egress. First, the capsids bud from the inner nuclear membrane and thus acquire an envelope. The steps following primary envelopment of the capsids have been controversial. One model suggests that the capsids carrying the nuclear envelope follow the secretory pathway to exit the cell. Another model for viral egress includes the fusion of the primarily enveloped capsid with the outer leaflet of the nuclear membrane or the endoplasmic reticulum (ER). This second fusion event would lead to loss of the primary envelope and tegument. To follow, the final envelopment and acquisition of tegument would occur in cytoplasmic compartments. This model, also known as the two-step envelopment model, has been highly supported with morphological and biochemical data (144). Finally, the enveloped virion leaves the host cell either by lysis of the infected cell during lytic infection or through budding from the host cell plasma membrane.

In addition to lytic, destructive infections, herpesviruses are capable of establishing latent infections within host cells. During this stage of infection, limited gene transcription occurs, with very few, if any, viral proteins being made. Through

repression of the full lytic cycle, no new virions are generated, and thus, the virus exists in a state of quiescence. When infecting cells that rapidly divide, the genome of herpesviruses is maintained as an episome within latently infected host cells, ensuring that the viral DNA is replicated and passed along to progeny cells. This maintenance of viral genomes provides a continual source of potentially infectious virus (219).

Reactivation of the virus from this latent state of infection to a productive lytic infection is unclear, but some triggers have been identified. For example, exposure to ultra violet (UV) light, heat, and physical or emotional stress, has been associated with the promotion of the lytic replicative cycle (74). Notably, due to latency, herpesvirus infections are maintained for the remainder of the lifetime of the host.

d. Human herpesvirus and disease

Due to differences in host cell susceptibility to infection, diseases presented by human herpesvirus infections differ. HSV-1 and HSV-2 occur worldwide and characteristically cause localized cutaneous lesions of mucosal sites of the mouth and genitals, respectively. While not undergoing lytic replication, HSV-1 and HSV-2 are neurotropic and remain latent in trigeminal ganglia. Rarely, HSV-1 and HSV-2 are also associated with meningitis and encephalitis (226). VZV primary infection results in systemic disease associated with the appearance of skin lesions (chicken pox) and normally occurs during childhood. Reactivation of VZV from latently infected ganglia results in herpes zoster (shingles), a painful, vesicular rash associated one or more dermatomes (12).

Pathogenicity of betaherpesviruses varies widely, with human cytomegalovirus (HCMV) being more pathogenic than HHV-6, and HHV-6 being more pathogenic than HHV-7 (96). Unlike infections with alphaherpesviruses that result in the establishment of latency within neurons, latency from betaherpesvirus infections can occur in many cell types (202). HCMV is prevalent in ~60% of adults in developed countries and in nearly all adults from developing countries (96). Following infection, HCMV can be isolated from bodily secretions, which allows for vertical and horizontal transmission despite lack of clinical symptoms (128). HCMV is also associated with iatrogenic transmission, through blood transfusions and organ transplants. Immunocompromised individuals often display HCMV-associated diseases including retinitis and pneumonitis. HHV-6, a ubiquitous betaherpesvirus (>85% of population), was first isolated in 1986 and is an etiological agent of exanthem subitum (roseola) and febrile seizures (96, 131). Additionally, HHV-6 has been demonstrated as neurotropic, and thought to be associated with the development of multiple sclerosis, however, direct involvement has not been demonstrated (51). HHV-7 is closely related to HHV-6, and was first isolated in 1990. HHV-7 is also a ubiquitous betaherpesvirus, but despite its wide-spread distribution, HHV-7 has not been associated with human diseases except for some cases of exanthem subitum (96, 131).

Epstein-Barr virus (EBV) is a ubiquitous gammaherpesvirus that is associated with adolescent infectious mononucleosis and with various malignancies. In the immunocompetent host, most infections are asymptomatic, but do result in lifelong latent infections within B cells (235). Some B cell malignancies have been highly

associated with EBV, especially within the immunosuppressed host, including post-transplant and AIDS patients. The tumors associated with these cases include Burkitt's lymphoma, Hodgkin's disease, nasopharyngeal carcinomas and central nervous system lymphomas (7). Interestingly, Burkitt's lymphoma is also endemic among children in areas of Africa and New Guinea (235).

The most recently discovered human herpesvirus is the gammaherpesvirus human herpesvirus-8 (HHV-8), also referred to as Kaposi's sarcoma-associated herpesvirus (KSHV). This virus displays unique global distribution, with approximately 40% of those living in sub-Saharan Africa positive for HHV-8 antibodies, and 10-25% of those in the Mediterranean possessing antibodies for the virus (1, 6, 9, 44, 59, 194). For the remainder of the world, only 2-5% of the population are seropositive for HHV-8, however, populations of HIV-1 positive individuals, seroprevalence can rise to 20-50% (1). Additionally, homo- or bisexual men have the highest risk of developing KS, not considering geography or ethnicity of individuals (20, 100, 185). Diseases positively associated with HHV-8 include Kaposi's sarcoma (KS), and two B cell malignancies, primary effusion lymphoma (PEL) and multicentric Castelman's disease (MCD) (2).

e. Primary immune response to herpesvirus infection

i. General characteristics

The human host has evolved to offer two means of protection against invading pathogens, including herpesviruses. Specifically, the immune system provides two

arms of immunity: innate and adaptive. The innate immune response is largely mediated by phagocytic cells and offers generalized, non-specific immune surveillance. Here, cells of myeloid lineage, including monocytes, macrophages, neutrophils, and dendritic cells, non-specifically phagocytize invading pathogens and can successfully clear them from the host. Phagocytic cells also play an important role in the generation of an inflammatory response to pathogens. Activated phagocytic cells secrete pro-inflammatory cytokines (IL-1, IL-8, TNF, IL-6, IL-12), which serve to recruit more phagocytic cells to the site of infection (106). In addition to phagocytic cells, the innate arm of the immune system maintains surveillance for invading pathogens using Toll-like receptors (TLRs). Originally identified based upon homology with the Toll receptor from *Drosophila* (141, 179), eleven TLRs have now been identified in humans, recognizing a wide variety of bacterial and viral pathogens (reviewed in (207)). To correlate with their patrolling function, TLRs are largely expressed on cells that are likely to first encounter pathogens including the phagocytic cells, macrophages, neutrophils, and dendritic cells (48, 49, 67, 141, 179, 208, 237). Activation of TLRs in response to virus infection is believed to occur through recognition of double-stranded RNA, single-stranded RNA, deoxycytidylate phosphate deoxyguanylate (CpG) DNA motifs, and envelope glycoproteins. With regard to human herpesviruses, TLR9 is activated by CpG DNA motifs found in the genomes of HSV-1 and HSV-2 (123, 137), and TLR2 is activated by HCMV and HSV-1 through interactions with viral glycoproteins, and through an unknown mechanism, respectively (53, 124). Following ligation, TLR9 elicits a signaling cascade that results in the secretion of the type I interferon (IFN), IFN- α . Type I IFNs

serve as antiviral molecules, activating components of the innate and adaptive immune response, including antigen-presenting cell (APC) maturation and the production of cytokines which activate B lymphocytes, T lymphocytes, and NK cells (212). Signaling from activated TLR2 results in the production of pro-inflammatory cytokines, including IL-6, that will recruit effector cells to the site of infection (53, 124).

If the innate response is insufficient in clearing invading pathogens, pathogen specific antigens produced within the host will trigger adaptive immune responses. For a period of several days (~5 days), antigen-specific T and B lymphocytes will proliferate and differentiate into effector cells that will act to clear the pathogen from the host. To begin the activation process of lymphocytes, antigen presenting cells, such as dendritic cells (DCs), transport antigen to local lymphoid organs and present this antigen to naïve CD4⁺ T lymphocytes in the context of HLA class II. CD4⁺ T lymphocytes recognizing this antigen are then primed and will differentiate into effector T lymphocytes. The cytokine environment of the naïve CD4⁺ T lymphocytes during their exposure to antigen will affect which class of effector T lymphocytes is generated, either T_H1 or T_H2. Once a subset of T_H lymphocytes dominates an immune response, production of the other subset is inhibited. Secretion of IL-12, TNF, or IFN- γ from antigen presenting DCs will result in the production of T_H1 CD4⁺ T lymphocytes, while naïve CD4⁺ T lymphocyte stimulation in the presence of IL-4 and IL-6 from DCs will result in the development of T_H2 CD4⁺ T lymphocytes. T_H2 effector T lymphocytes will remain in the lymphoid organs to stimulate humoral immunity through activation of B cells, while T_H1 travel to sites of infection,

stimulating cell-mediated immunity. Specifically, T_H1 lymphocytes activate $CD8^+$ cytotoxic T lymphocytes and macrophages through secretion of $IFN-\gamma$ and other proinflammatory cytokines. Activated $CD8^+$ cytotoxic T lymphocytes will then eliminate infected cells displaying virus-specific antigens in the context of HLA class I. Working together, both branches of the immune system work together to rid the host of invading pathogens and establish effective protective immunity to prevent re-infection with the same pathogen (106).

As herpesviruses establish life-long latency within their host, the immune system must be circumvented. Indeed this is the case as herpesviruses express many immunomodulatory proteins. For example, a herpesvirus encoding a protein that negatively controls macrophage activation would be spared from the inflammatory response that normally results in viral clearance (80). In fact, HHV-8 and RRV encode homologues of CD200, which reduce macrophage secretion of the pro-inflammatory cytokine TNF, blocking the development of T_H1 cells and the cell-mediated immune response. More detail regarding CD200 and viral CD200 homologues action are discussed in later sections.

ii. Human gammaherpesvirus specific immunity

The fact that EBV infection is ubiquitous and only a small fraction of these individuals develop EBV associated malignancies suggests a critical role for the immune system in controlling viral infection (235). To control primary infection with EBV, cytotoxic $CD8^+$ lymphocytes (CTLs) play an important role in eliminating virus infected B lymphocytes (31, 32), although, a small proportion of infected B

lymphocytes will become latently infected (235). Long-term control of viremia is achieved through recognition of latently infected B lymphocytes by CD8⁺ T lymphocytes in a CD4⁺ T lymphocyte dependent manner (3, 108, 176). The importance of CD4⁺ T lymphocytes is highlighted in HIV/EBV co-infected patients experiencing CD4⁺ T lymphocyte depletion. Specifically, CD4⁺ T lymphocyte depleted patients have a higher propensity for developing EBV associated malignancies in comparison to other individuals infected with EBV (7, 37, 55, 114, 151). In addition, administering T lymphocyte therapy to immunosuppressed patients has proven effective in controlling EBV associated malignancies (7, 165).

Immunosuppression administered to organ transplant patients to control graft versus host disease also echoes the importance of cellular immunity in controlling EBV infection. 90% of post-transplant lymphoproliferative disease (PTLD) results from the lack of EBV-specific cellular immunity. The first line of defense against PTLD is to restore this immune surveillance through the reduction of the dosage of immunosuppressing agent (30, 94). Cellular immunotherapy has also proven effective in controlling PTLD. Specifically, EBV-specific CTLs administered through adoptive transfer clear EBV infected cells responsible for the development of PTLD (101, 180).

Similarly, the importance of cell-mediated immunity in controlling HHV-8 viremia is realized in the immunocompromised patient. HHV-8 associated malignancies, like EBV associated malignancies, are most prevalent in patients that are immunocompromised from HIV infection or from iatrogenic means (2, 25, 191). It understood that HIV infection results in depletion of CD4⁺ T lymphocyte

populations (37, 117), which allows for unchecked replication of HHV-8. Specifically, without CD4⁺ T lymphocyte help, the cytotoxic CD8⁺ T lymphocytes that work to control viral replication are unable to become activated and mount a response against infected cells (162, 220, 221). Administering highly active antiretroviral therapy (HAART) to HIV/HHV-8 co-infected individuals reduces HIV viral loads, which can lead to the reconstitution of depleted CD4⁺ lymphocyte populations, and reduced incidence of HHV-8 associated malignancies, further implicating CD4⁺ T lymphocyte help for CD8⁺ T lymphocyte control of HHV-8 replication (27, 168, 173, 222, 228).

2. Human herpesvirus 8 (HHV-8)/Kaposi's sarcoma-associated herpesvirus (KSHV)

a. Identification and classification of a Kaposi's sarcoma-associated herpesvirus

Kaposi's sarcoma-associated herpesvirus (KSHV) was first identified by Chang *et al.* in 1994. In this study, two viral DNA fragments were detected in Kaposi's sarcoma (KS) tissues from a patient with acquired immunodeficiency syndrome (AIDS) (42). As this virus was the eighth identified herpesvirus found to infect humans, it was given the formal name human herpesvirus 8 (HHV-8). Upon further analysis, HHV-8 DNA was found in >90% of AIDS-KS lesions and in AIDS-associated body cavity-based non-Hodgkin's lymphomas (42). It was also determined that HHV-8 is the etiological agent of non-AIDS KS lesions (148).

Phylogenetic analysis of the major capsid protein revealed that HHV-8 is a member of the *Rhadinovirus* (gamma-2) genus within the gammaherpesvirus subfamily, and is closely related to herpesvirus saimiri (HVS), and more distantly related to the gamma herpesvirus Epstein-Barr virus (EBV). While HHV-8 is the first member of its genus known to infect humans, HVS can infect and immortalize human T cells. Natural infection with HVS occurs in squirrel monkeys (*Saimiri sciureus*) where it is associated with T cell lymphomas (142, 177, 225). Another member of the *Rhadinovirus* genus, rhesus rhadinovirus, was isolated from rhesus macaques (*Macaca mulatta*), and is found to be more closely related to HHV-8 than HVS (61, 195). Sixty-six of the 85 HHV-8 open reading frames (ORFs) are co-linear with EBV and HVS, indicating that these genes are likely to behave similarly to their counterparts in the other gammaherpesviruses (149). The HHV-8 genome has one long unique region (LUR) flanked by terminal repeats with 84.5% G+C content. The LUR contains all of the identified ORFs, and is approximately 140.5 kb, with 53.5% G+C content (184). More recently, the three-dimensional structure of HHV-8 virions has been investigated and was found to closely resemble those of herpes simplex virus type 1 and human cytomegalovirus (232).

b. HHV-8 associated diseases

i. Kaposi's sarcoma (KS)

Kaposi's sarcoma (KS) was first described in 1872 as "idiopathic multiple pigmented sarcomas of the skin," by the Hungarian dermatologist Moritz Kaposi

(111). Today, KS is recognized as the most common neoplasm in patients with AIDS (20, 175). In addition to AIDS-associated KS, three other forms of KS exist: classic, endemic, and iatrogenic or post-transplant. Classic KS is predominately observed in elderly patients of Southern European, Arabic, or Jewish ancestry (78). Endemic KS is found primarily in equatorial countries of Africa, and has existed for many years. This aggressive form of KS can be found in adults as well as children, and affects the lymph nodes (56, 161). Immunosuppression associated with organ transplantation is believed to increase the incidence of KS, especially in regions where endemic and classic forms are prevalent (98, 167, 171). Notably, AIDS-KS is the most aggressive of the four forms, where lesions are found disseminated in skin and visceral organs including the lungs, gastro-intestinal tract, liver, and spleen (79, 100).

KS is described as a multifocal angioproliferative disease. Histologically, early KS lesions largely consist of blood vessels and scattered spindle-shaped cells. As progression of KS lesions ensues, these spindle cells proliferate and become the predominate cell type in advanced (nodular) KS lesions (86, 174) (Figure 1.2A). Most spindle cells express endothelial cell markers (CD31 and CD34), therefore, spindle cells are believed to be of endothelial cell origin (68, 183). In addition, increased levels of T helper type 1 (T_H1) cytokines and growth factors have been detected in KS lesions, including $IFN-\gamma$, TNF, $IL1\beta$, IL-2, IL-6, basic fibroblast growth factor (bFGF), vascular endothelial cell growth factor (VEGF), which support vascularization and cell proliferation within KS lesions (70, 75, 145, 189). The presence of these proinflammatory cytokines upregulates expression of intracellular adhesion molecules in microvascular endothelial cells and spindle cells (104, 105),

which is responsible for enhanced adhesion and tissue extravasation of lymphocytes, monocytes to KS lesions. Proinflammatory cytokines also induce inflammation and angiogenesis in an autocrine manner as KS cells express some corresponding receptors for these cytokines (143, 190). HHV-8 proteins also aid in the establishment and proliferation of KS lesions, including viral IL-6 (vIL-6), viral macrophage inflammatory proteins (vMIPs), and the viral G protein-coupled receptor (vGPCR), that promote angiogenesis within lesions (191). In addition, vMIPs are important chemoattractants for T_{H2} T cells (vMIP-I and -III) (69, 203), eosinophils (vMIP-II) (23), and monocytes (vMIP-I and -II) (154), further contributing to the pathobiology of KS lesions (63). A more detailed description of viral genes associated with pathogenesis follows in a later section. HHV-8 DNA is also detected in KS lesions, from peripheral blood mononuclear cells (PBMCs), and from plasma isolated from KS patients utilizing polymerase chain reactions (PCR) with primers specific for viral sequences (2).

All possible patterns of clonality have been identified within KS lesions isolated from various patients (86). Therefore, whether KS lesions initiate as a single malignant cell or multiple cells is unclear. One likely possibility of KS development is that KS begins as a polyclonal hyperplastic lesion that, when under selective pressure or host immunosuppression, gives rise to a clonal cell population (2). In fact, this type of disease development is observed in post-transplant patients, in which EBV enhances B cell proliferation to drive polyclonal hyperplasia to monoclonal tumors (119). Further, the idea that KS does not begin as a monoclonal lesion is supported by the fact that HHV-8 is present in fewer than 10% of spindle cells of

early KS lesions, while later stages of the lesions, >90% of spindle cells are latently infected with HHV-8 (68).

KS-derived cells lines have been developed and have confirmed the spindle-shaped cell phenotype along with the tumorigenicity, angiogenicity, and metastatic potential of these cells. However, these cells rapidly lose the HHV-8 genome when cultured *in vitro*, making them undesirable for use in studies of viral transcription or viral protein production (19, 76, 129, 130, 136).

ii. Primary effusion lymphoma (PEL)

Extensive studies have been performed to link the presence of HHV-8 with the development of PEL in HIV seropositive and seronegative patients (Figure 1.2B) (35, 36, 82, 84, 112, 152, 163, 187). Certain criteria have been established for the designation of lymphomas as PEL. These include, but are not limited to (i) localization of a lymphomatous effusion in the pleural, peritoneal and/or pericardial cavity in the absence of a solid tumor mass, distinguishing PELs from other non-Hodgkin's lymphomas that originate systemically or in the central nervous system (113, 118, 120, 121); (ii) cells are of B cell origin with clonal immunoglobulin gene rearrangements, but lack expression of B cell antigens and immunoglobulin; (iii) cells express CD45 and one or more activation-associated antigens; (iv) a lack of mutations within the oncogenes *c-myc*, *bcl-2*, *ras*, and *p53* gene sequences. In addition, coinfection with EBV is observed in most (86%), but not all, PEL (152). Terminal repeats of HHV-8 DNA isolated from two PEL cell lines isolated from the same

tumor have been shown to be identical, suggesting that one copy of the virus infects the lymphoma progenitor cell, followed by clonal expansion (191).

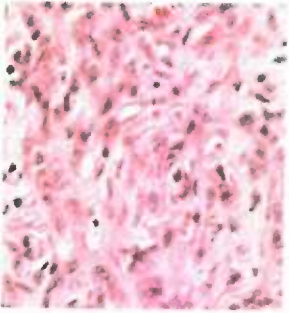
While PEL are very rare malignancies, accounting for only approximately 3% of AIDS-related lymphomas, they are associated with poor prognosis. Patients diagnosed with PEL have a median survival time of only five months (35). The only cell lines that are capable of maintaining the genome of HHV-8 are those of PEL origin. Of these cell lines, those lacking EBV are most relevant for studying HHV-8 biology and include BCBL-1, BCP-1, KS-1, and BC-3 (11, 24, 34, 40, 81, 178, 188).

iii. Multicentric Castleman's disease (MCD)

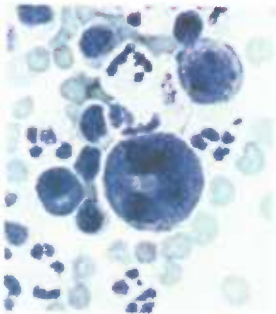
In addition to PEL, another lymphoproliferative disorder linked with HHV-8 is multicentric Castleman's disease (MCD) (Figure 1.2C) (200). Castleman's disease (CD) is a polyclonal, neoplastic disorder that can be divided into two forms depending on the degree of vascularization and B cell hyperplasia: hyaline-vascular and plasma cell variants. While these two types of CD are discrete, they can both be present within the same patient and both can occur in HIV-negative and HIV-positive patients (160, 200), although those with the plasma cell variant are more likely to develop KS and non-Hodgkin's lymphoma (NHL). Patients with plasma cell types of CD display generalized lymphadenopathy, and multiple lymphadenopathies, giving rise to the "multicentric" nature of MCD (54). MCD was first identified as a benign malignancy (38), however, MCD patients seropositive for HHV-8 and HIV are at an increased risk of developing malignant lymphomas (159), thereby associating HHV-8⁺/HIV⁺ MCD patients with poor prognosis (68).

Figure 1.2 (A) Histological section of KS lesion stained with hematoxylin and eosin. Note presence of spindle cells and abundant vasculature. (B) Wright-Giemsa stain of a preparation of PEL cells. Tumor cells are of larger size relative to benign cells. (C) Hematoxylin- and eosin-stained lymph node section taken from an HIV-positive patient with MCD. Here, a large follicle is shown with a large, concentrically arranged mantle zone surrounding a germinal center. *Figures and legend adapted from (2)*

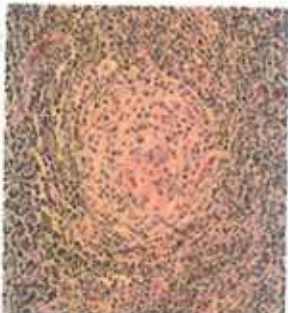
A.



B.



C.



c. Viral genes associated with pathogenesis

Through evolution with their host, herpesviruses have pirated many cellular genes for their benefit (156, 157, 184). In the case of HHV-8, these genes include a viral cyclin D homologue (vCYC) that acts to bypass cellular cycling blocks to promote cellular proliferation (41, 43), a bcl-2 homologue, and a viral FLICE inhibitory protein (vFLIP), which block TNF, Fas, and mitochondrial-mediated routes of apoptosis (22, 46, 192, 213). In addition, HHV-8 encodes cytokine homologues, including an interleukin-6 (IL-6) homologue, which has been demonstrated to enhance B cell proliferation, as well three chemokine homologues, viral macrophage inflammatory proteins (vMIP-I, -II, and -III) (147). HHV-8 infected cells also express an IL-8—like receptor (viral G-protein coupled receptor [vGPCR]), which has been extensively studied, and has been reported to promote cellular transformation through its constitutive signaling activity (10, 13, 41, 97). To evade host immune responses, HHV-8 encodes various immunomodulatory proteins. These include vCD200, a viral homologue of cellular CD200, which abrogates macrophage activation (77), viral interferon regulatory factors (vIRFs), that function to block interferon-mediated signaling (83, 132, 210, 211, 240), and complement-binding proteins (CD21/CR2) that block complement activation (184). Taken together, these viral homologues work together to promote viral replication and the survival of cells harboring HHV-8.

d. Models for studying HHV-8

As HHV-8 only infects human hosts, *in vitro* and alternate *in vivo* models of infection are required for understanding the biology of this virus. To date, B lymphocyte cell lines derived from PELs have been extensively utilized in the laboratory for *in vitro* studies. These cell lines carry HHV-8 primarily in the latent state, but can be induced to undergo lytic replication by the addition of phorbol esters, including 12-*O*-tetradecanoylphorbol-13-acetate (TPA) (178). Upon lytic induction, these cell lines can be used as an *in vitro* model of lytic HHV-8 infection, facilitating the categorization of open reading frame expression. These cell lines would also be useful to assess efficacy of antiviral therapeutic agents as potential *in vivo* treatments of HHV-8 associated diseases. In addition to the latently infected lymphocyte cell lines, a model of *de novo* HHV-8 infection of immortalized human endothelial cells has been established and may help to determine processes involved in cellular transformation (150).

To examine viral factors involved in pathogenesis, animal models are most effective. Murine gammaherpesvirus 68 (MHV-68) is currently utilized as a mouse model of HHV-8 infection, as these two viruses share the same gamma-2 herpesvirus subfamily classification and significant sequence homology (196). Although MHV-68 establishes latency in B lymphocytes as does HHV-8 (206), the genome of MHV-68 lacks several ORFs that are likely critical to the pathogenesis of HHV-8. HHV-8 proteins not encoded by MHV-68 that may be involved in HHV-8 pathogenesis include vFLIP, vCD200, vIRF, vMIP, and vIL-6 (196). Therefore, MHV-68 may act differently during acute and latent infections due to variation in gene content, and is a substandard model for examining *in vivo* HHV-8 infection. More recently, a gamma-

2 herpesvirus was isolated from a simian immunodeficiency virus infected rhesus macaque (*Macaca mulatta*) displaying lymphoproliferative disorder (LPD) (195). Upon sequence analysis, it was revealed that this non-human primate virus, rhesus macaque rhadinovirus (RRV), is very similar to HHV-8. Specifically, RRV shares 67 of its 79 ORFs with HHV-8, and importantly, these ORFs include many of those believed to be important for pathogenesis of HHV-8 (5, 195). In addition, the rhesus macaque host is more closely related to humans genetically than is a mouse, and therefore, insights into the immune response to RRV infection within the rhesus macaque will likely resemble more closely what occurs during HHV-8 infection in humans. Other gamma-2 herpesviruses have also been isolated from other non-human primates such as chimpanzees and gorillas (95, 125, 126), but these animals are less practical than the rhesus macaque as experimental hosts as they are less abundant for research purposes and more expensive to maintain.

3. Membrane proteins with immunoglobulin superfamily domains

a. Characteristics

Membrane proteins containing immunoglobulin superfamily (IgSF) domains are the most abundantly expressed proteins on the surface of leukocytes (16). As the adaptive arm of the immune system has developed, the number of molecules containing these domains has increased and this is represented when comparing the abundance of genes expressing IgSF-containing proteins in *Drosophila* (172) with

those found in humans (127, 217). Structurally, IgSF domains are constructed of two beta sheets of antiparallel strands held together by a disulfide bridge (Figure 1.3) (8). Immunoglobulin domains are categorized into one of two types: variable (referred to as V-like), or constant (referred to as C-like). While sequence patterns of IgSF domains resemble those of the V-like domains, the size of IgSF domains is more similar to those of the shorter C-like domains (15). A protein may contain as many as 17 IgSF domains and as few as one, but the majority of IgSF proteins contain two as this maintains the optimal distance between two interacting cells (15, 227). In addition, most membrane proteins with IgSF domains are type I membrane proteins and are glycosylated to varying extents (15).

b. Interactions

It is accepted that IgSF domains function primarily in cell-to-cell recognition and communication, likely through interactions with other IgSF domains. These interactions have been characterized as weak. For example, an interaction between two IgSF domain containing proteins may be approximately 1000 times weaker than those observed between antibody molecules binding protein antigens. There is great diversity as to the nature of the cytoplasmic regions of membrane proteins containing IgSF domains. Upon engagement, some of these proteins have the capability of eliciting a signaling cascade through identified motifs such as immunoreceptor tyrosine-based inhibitory motif (ITIM) and immunoreceptor tyrosine-based activation motif (ITAM). Others are part of complexes that associate with membrane proteins which will lead to signaling upon engagement of the IgSF domain-containing protein

(15). Taken together, interactions between membrane proteins containing IgSF domains can result in a wide array of cellular responses, due to activation or inhibition of one or a number of cellular pathways.

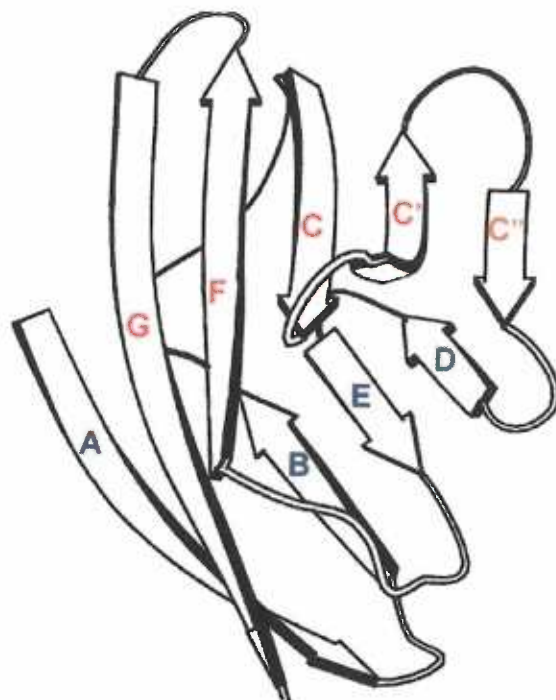
4. CD200

a. Characteristics

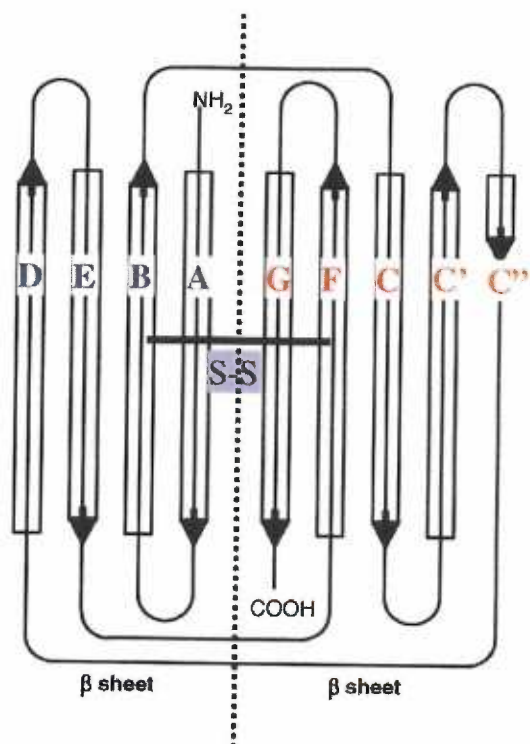
CD200, formerly known as OX2, is a type I membrane glycoprotein that has two IgSF domains. Originally identified within rodent models, CD200 is expressed on the surface of a wide variety of cells including neurons, epithelium, and lymphoid cells (14). As this protein has a short (19 amino acids) cytoplasmic domain lacking identifiable signaling motifs, it is unlikely to generate intracellular signals itself, but may instead elicit its effects through binding of a receptor on another cell. The receptor for CD200 has been identified and is termed CD200 receptor (CD200R). Like CD200, CD200R also contains two IgSF domains, but has a restricted expression pattern in that it is largely expressed on the surface of myeloid cells (230). Flow cytometric analyses have revealed high levels of CD200R expression on peripheral blood T cells (CD8⁺ and CD4⁺), neutrophils, and basophils. Human monocytes from peripheral blood expressed CD200R at more moderate levels, however, upon differentiation of monocytes into dendritic cells (DCs) *in vitro*, the levels of CD200R are increased. Human macrophages from skin were also found to express moderate levels of CD200R. Murine CD200R shares similar expression

Figure 1.3 (A) Typical Ig-fold showing the beta strands as broad arrows and loops joining them as thin tubes (B) Schematic view of the topology of strands and loops. In C-like domains, the C' and C'' strands are missing. The position of the conserved disulfide bond is indicated by S-S between strands B and F. *Figure adapted from (15).*

A.



B.



patterns as the human receptor on cells from peripheral blood, but higher levels of CD200R are found on murine monocytes and splenic macrophages (230). A summary of human and murine CD200R expression is presented in Table 1.1.

b. CD200-CD200R interaction

Epitopes within CD200 and CD200R that are involved in their interaction have been identified. Both proteins utilize their N-terminal IgSF domains for functional interaction (45, 99, 170). Upon examination of the signaling capabilities of CD200R, phosphotyrosine-binding (PTB) motifs (NPXpY) have been identified within the cytoplasmic domain (231, 238). Signaling as a result of CD200R ligation by CD200 has been studied in the case of murine CD200R expressed on murine mast cells. Incubating mast cells with soluble murine CD200 prevented the degranulation of these cells (155), confirming the negative regulatory function of murine CD200 in this system. Through investigating the molecular mechanisms of CD200-mediated inhibition of mast cell activation, it was revealed that murine CD200R engagement results in tyrosine phosphorylation (Y²⁹⁷) of the receptor and subsequent binding of tyrosine-phosphorylated PTB domain binding proteins, Dok1, and Dok2, which subsequently recruit Ras GTP-ase activating protein (GAP) to the receptor complex. In addition, tyrosine-phosphorylated Src homology 2-containing inositol 5'-phosphatase (SHIP) is recruited specifically by Dok1, although the function of this protein in association with CD200R is unknown (238). Association of Dok1 with RasGAP has been demonstrated to reduce Ras activity, resulting in the inhibition of

mitogen-activated protein kinase (MAPK) pathways in B and mast cells (164, 233). Indeed, triggering CD200R on murine mast cells rapidly leads to inhibition of extracellular signal-regulated kinase (ERK) activation. Activation of the Ras-independent pathways, p38 MAPK and Jun N-terminal kinase (JNK), is also blocked following CD200R ligation (238). While the signaling cascade has not been examined for human CD200R, the tyrosine at position 297 is conserved, which may suggest similar outcomes as a result of receptor ligation. A summary of signaling cascades arising from murine CD200R ligation is depicted in Figure 1.4.

As expression patterns would suggest, ligation of CD200R largely affects monocyte, macrophage, and microglial functions. Therefore, the possibility exists that processes carried out by these cell types would be interrupted upon CD200R engagement and subsequent signaling. Much of what is understood for the function of CD200 was learned from the use of C57B6 mice lacking CD200 (CD200^{-/-}). While these mice developed normally and displayed normal behavior, they differed from wild-type mice in that they demonstrated an increase in number and activation state of CD200R⁺ macrophages, microglia, and dendritic cells (102). Taken together, these data imply that CD200 supplies inhibitory signals to cells expressing CD200R and reducing activation of these cells that are important for innate immunity (106). To further test the idea that CD200 negatively regulates cells of myeloid lineage, two autoimmune models of disease were assessed in CD200^{-/-} mice: experimental autoimmune encephalomyelitis (EAE), and collagen-induced arthritis (CIA), both of which are believed to be mediated by activated macrophages. Interestingly, CD200^{-/-} mice displayed an earlier onset of EAE, and susceptibility to CIA, which does not

Tissue	hCD200R	mCD200R
Monocytes	++	+++
Granulocytes	+++	+++
Dendritic cells	+++	+
Macrophage	++	+++
Mast cells	+	++
T cells	++	++
T cell clones Th1	+	-
T cell clones Th2	++	+
B cells	+/-	+
NK cells	-	-
NKT	+	+

Table 1.1 Summary of distribution of human (h) and murine (m) CD200R. Data are compiled from quantitative RT-PCR and flow cytometry. *Table adapted from (230).*

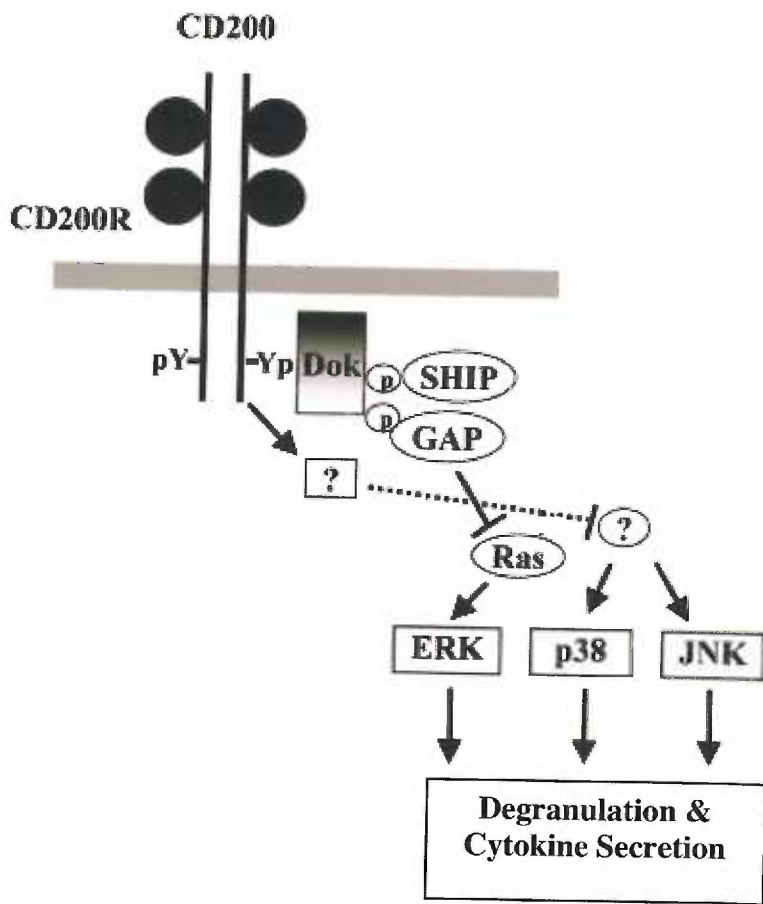
affect wild-type C57B6 mice (102). In addition, the frequency of CIA observed in susceptible mice could be reduced through the administration of either agonistic anti-CD200R antibodies or soluble CD200-Fc, further implicating the inhibitory nature of CD200-CD200R interaction (91). In addition, enhanced microglial activation was confirmed through utilizing the facial nerve transection model, where the microglial response of CD200^{-/-} mice was accelerated in comparison to wild-type mice (102). Induction of immune tolerance is also supported in rodent transplant models (87, 89, 90, 92). In comparison to untreated mice, those receiving pre-transplant donor DCs expressing CD200 demonstrated higher success in allograft survival (87). Further, this protective effect was abolished through the administration of an antibody specific for CD200 (87). To examine immune regulatory roles of CD200 *in vitro*, CD200R⁺ splenocytes were incubated with CD200 expressed on DCs or expressed as a soluble protein. Following incubation, CD200R⁺ cells shifted to a type 2 cytokine profile, while reducing expression of type 1 cytokines (87).

As CD200 is also expressed on cells of the trophoblast (28), the importance of CD200 in blocking fetus rejection has been identified. It appears that expression of CD200 at the feto-maternal interface is important in regulating cytokine production from infiltrating macrophages, altering this from a type 1 cytokine-rich environment to one with a larger proportion of type 2 cytokines (52). It is this regulation of cytokines that is important in maintaining a successful pregnancy.

c. Viral CD200 homologues

As CD200 suppresses activation of macrophages, it is logical that a virus that

Figure 1.4 Proposed model for CD200R-mediated inhibition of mast cell activation. Triggering CD200R by CD200 induces its phosphorylation and recruitment of Dok1 and Dok2. Dok1 and Dok2 are phosphorylated and bind to RasGAP and SHIP, which leads to inhibition of Ras and ERK activation. Other unknown molecules may mediate the inhibition of p38 MAPK and JNK activation. *Figure and legend adapted from (238).*



evolves with its host would have a selective advantage if it could express CD200 on the surface of infected cells. Indeed, viral CD200 (vCD200) homologues have been identified in various virus families including herpesviruses, poxviruses, and an adenovirus. More specifically, these homologous proteins are predicted to be encoded by RRV R15, HHV-8 K14, HHV-6 U85, HHV-7 U85, the English strain of rat cytomegalovirus e127, Yaba-like disease virus 141R, Yaba monkey tumor virus Yb-C2R, lumpy skin disease virus LSDV138, Shope fibroma virus S141R, myxomavirus M141R, sheep pox virus ORF138, and duck adenovirus ORF4 (218). Comparing the V-like domains of these viral homologues with CD200, the relatedness to CD200 structure is evident, as the beta sheets characteristic of the Ig fold are retained in the homologous proteins (Figure 1.5) (77).

To date, the only vCD200 homologues that have been analyzed in terms of function are those encoded by myxoma virus M141R (33) and HHV-8 K14 (77). Both of these proteins have been demonstrated to resemble human CD200 in their ability to control macrophage activation. Deletion of myxoma M141R from the genome of myxoma virus had no effect on *in vitro* viral growth properties; however, the importance of this molecule in controlling the host immune response was underscored from *in vivo* studies. Specifically, infection of European rabbits with myxoma virus lacking M141R resulted in complete recovery of the animals, while all rabbits infected with wild-type myxoma virus were declared moribund and euthanized at day 9 post infection (33). The viral CD200 homologue encoded by HHV-8 will be the focus of the next section.

5. HHV-8 encoded viral CD200 homologue

a. Function

Based upon initial studies of HHV-8 vCD200, this protein was believed to elicit a pro-inflammatory response from monocytes, macrophages, and DCs. This study utilized a soluble form of HHV-8 vCD200, where the predicted extracellular domain was fused to glutathione-S-transferase (GST) in addition to a stable B cell line expressing HHV-8 vCD200 to elucidate the function of this protein. In this study it was reported that when incubated with GST-HHV-8 vCD200 or with B cells expressing HHV-8 CD200, cells of myeloid lineage demonstrated an increase in production of the type 1 cytokines interleukin (IL)-1 β , IL-6, monocyte chemoattractant protein 1, and tumor function. In addition, it was also demonstrated that HHV-8 vCD200 is expressed on the surface of latently infected B cells following lytic induction and that HHV-8 vCD200 was also capable of binding human, rat, and mouse CD200R with nearly identical kinetics and affinity as human CD200 (77).

b. Transcription of HHV-8 K14

Transcripts containing K14 have been detected at early time points during HHV-8 lytic infection. More specifically, Northern blot analyses with RNA from latently-infected PEL cell lines treated with phorbol esters to induce lytic replication have revealed that K14 is the upstream ORF of a ~2.8 kb bicistronic transcript with ORF74 which encodes the vGPCR (47, 116, 153, 209). Further investigation of this

bi-cistronic transcript revealed that there is a splicing event that takes place between these two ORFs, which removes 149 bp of sequence. Importantly, this splicing event does not appear to alter expression of either protein as the entire sequence of each ORF is maintained (116, 153). Expression of vGPCR as the second ORF on this transcript is thought to occur through nonclassical means, such as the use of an internal ribosome entry site, or perhaps through leaky ribosomal scanning, or translational re-initiation. However, these proposed mechanisms of vGPCR expression have not been examined and are only speculative.

Other studies have sought to examine the presence of the K14/ORF74 transcripts in clinical samples. It was determined that this bi-cistronic message is present within PEL specimens, confirming that expression of K14 and ORF74 could be associated with HHV-8-associated disease progression (153).

c. Implications for vCD200 expression during infection

An HHV-8 infected cell would benefit from immune evasion, allowing for the establishment of a lifelong latent infection. To do this, HHV-8 has pirated a number of genes from its host and used them to its advantage in outsmarting the immune system. HHV-8 vCD200 is an example of this gene piracy. As K14, the ORF that encodes HHV-8 vCD200, is expressed at early time points during lytic infection (116), HHV-8 vCD200 could deliver an inhibitory signal to local CD200R⁺ myeloid cells, restricting TNF production from these cells that would otherwise initiate a cell-mediated immune response against the invading virus. More specifically, an infection with a virus lacking vCD200 would ideally promote a cell-mediated response that

Figure 1.5 Alignment of the predicted Ig V-like domains of CD200 and viral CD200 homologues. The sequences shown are as follows: human CD200, R15 from rhesus macaque rhadinovirus (RRV), K14 from HHV-8, U85 from HHV-6, U85 from HHV-7, 141R from Yaba-like disease virus (YLDV), Yb-C2R from Yaba monkey tumor virus (YMTV), LSDV138 from lumpy skin disease virus (Lumpy), S141R from Shope fibroma virus (SFV), M141R from myxomavirus (MV) strain Lausanne; sheep pox virus (SPOX) ORF138, and duck adenovirus (D adeno) ORF4. The bars predict the extent of the beta-strands characteristic of the Ig fold by comparison to solved structures. The cysteines that are thought to form an unusual F-to-G strand disulfide are in boldface, and residues identical in four or more sequences are boxed. *Figure adapted from (77).*

Host:CD200
RRVR15
HHV8 K14
HHV6 U85
HHV7 U85
YLDV141R
YMTV7b-C2R
SPVSI41R
MM/MI41R
Lumpy
SPOX38
Dadeno

--- QVQVVTQDERE-QLYTTASLRLCGLQNAQ-----EALLIVTWQKPKKAVSP-----ENMVTTFSENHG--
---ALQTHYAAYV-PVHSTASLQCCLLTPH-----DVLIVTWQKQESPSP-----VNVATVYSSSEAG--
---ARVQGPMRGSAALTCATTPRA-----DIVSVTWQKQOLPGP-----VNVAVLYSHSSYG--
.HFVLPHEITSPSLIYEIGSIVTTPHCRLLETTT-----NIRSSVSMYNKRLITSNHEVQNMMDNLSPTDDGY
---LYPIMHHRV-ELGNTIVRQCCTVDTTK-----NLSVWIMFHRVELLHNHT-INTKNLKNMSBK-
---QSTDCPFVKSFINSLDIKITCTKTSF-----NTIITWKKDNKFFIIAG-YOICGFVIL-
---QSTDCPVEY-QNSLIDAKITCTKIHSHS-----NTIITWKKDNKFFIIAA-YOICGFVIL-
---YAIYCTNTTVEY-HVNVVTISCNNTGSRDNDSSNRLTFHLITWKKDNK-----TVAGYVGL-
---YSVRCNTNTTVAE-HVNVVTISCNNTGSRDNDSSNRLTFHLITWKKDNK-----TTIAGYVGL-
NVILSASCISKIYSSFKENTVKISCNKTSKF-----NSIITWKKNE-----TTIATYGPHG
NVILSASCISKIYSSFKENTVKISCNKTSKF-----NSIITWKKNE-----TTIATYGPHG
TALCSQVDFRGPARLIVGSTGTFPHCSLPGNR-----DVLAITWKNNDTNVGA-----LIAATYGPHG

Host:CD200
RRVR15
HHV8 K14
HHV6 U85
HHV7 U85
YLDV141R
YMTV7b-C2R
SPVSI41R
MM/MI41R
Lumpy
SPOX38
Dadeno

---VVIQPAYKDKINITQL-GLQNSTITFWNITLEDDEGCYMCLEFNTFG-PQKISGTAACLTVYVQP
---TVPQPPAGRVDIPBH-KLTRITLKPFPNATLEDEGCYLCIFNAPFG-VGKLSGTAACLTVYVQP
---VVVQTOYRHRKANITCP-GLWNSTLVTHNLAYVDEDEGCYLCIFNSFG-GRQVSGTAACLEVTSPF
VLHELKLNKINNLAVDSKLYFHIKHNRTTSELKIAKASAYDATCLTCTFTVDN-EKTSATSSCLKLPMP
-IVHEF---KHRDKESIIFPNA-NNITALLKFKSRRTINDAGCLTCARPAKT--RLSITMSQVHLSMKP
---EKFQKILVVSXK-SPNESTILIKNVNIFDRGCYTCVFNPLVSKNNEKGVVCLT-
---NKFKQKIQVLSK-SPNESTILIKNVNIFDRGCYTCVFNPLVSKNNEKGVVCLT-
---PSGPAIQNKKIEYLSLST-QYNTSTILIKNVSAEDSSGLYYCIRFNSF--MPLSSEEGVVMVNTT
---PSGATIKDASKIEYLSLST-QYNTSTILIKNVSAEDSSGLYYCIRFNSF--MPLSSEEGVVMVNTT
---SSYVDDTKNKIEYISK-SPNYSTIVIKNATIQDNSCYTCIRNILL-SENDEKGTLCINTTND
---YVDDVYKNIKIEYISK-SPNYSTIILIKNATIKDNVYCYTCIRNILL-SKNDKGTLCINTTND
---VVRANGTALRITSN--SVTSLTLLNIIYYAVAGAVYTCIPNVVFP-DGAIISGHGVTGVVBDP

arose from activation of T_H1 cells. However, as the CD200/CD200R interaction is understood to reduce type 1 cytokine production from myeloid cells, this interaction would reduce cell-mediated immunity, allowing for viral replication and the establishment of latency (refer to section 1.e).

Interestingly, HHV-8 vCD200 is made from a bi-cistronic message along with ORF74, which encodes the viral GPCR. vGPCR expression in cell culture and in nude mouse models has been associated with transformation and angiogenesis, likely due to constitutive activation of mitogen-activated protein kinase pathways and vascular endothelial growth factor (VEGF) secretion (13, 146, 199). As only a small percentage (~1-2%) of cells within HHV-8 infected tissues are undergoing lytic replication, vCD200 and vGPCR could be functioning through paracrine mechanisms that promote formation of KS lesions (239). The secretion of VEGF from infected cells as a result of vGPCR expression has been well established, and would fit the model of paracrine modes of action, with VEGF binding to upregulated VEGF receptors on nearby infected cells (166), promoting angiogenesis within KS lesions. As lytic replication continues, the immune system needs to be regulated to ensure the completion of the viral lytic cycle. Therefore, one could envision that expression of HHV-8 vCD200 on the surface of infected cells could be involved in limiting activation of infiltrating macrophages and the subsequent cell-mediated immune response. Together, HHV-8 vCD200 and vGPCR could be involved in maintaining HHV-8 infection and promoting the transformation processes associated with KS development.

To definitively identify the roles of vCD200 during HHV-8 infection *in vivo*, an animal model of infection must be utilized. Here, the host will be infected with a virus lacking vCD200 expression to test the hypothesis that cells infected this mutant virus will be cleared at a higher rate due to activated cellular immunity, thereby reducing overall pathogenesis in comparison to infection with wild type virus. Since MHV-68 lacks a vCD200 homologue, another animal model of HHV-8 infection would need to be utilized. As RRV encodes a vCD200 homologue, infection of rhesus macaques with this rhesus macaque homologue of HHV-8, presents itself as the ideal model system for investigation of this hypothesis. Importantly, the construction of RRV lacking R15 must maintain proper expression of vGPCR to definitively prove a role for vCD200 in any disease development.

6. Rhesus macaque rhadinovirus (RRV): a nonhuman primate model for HHV-8 infection

a. Identification and classification of RRV

Two independent strains of rhesus macaque rhadinovirus (RRV) have been identified from rhesus macaques (*Macaca mulatta*) housed at different primate research centers: strain 26-95 from the New England Primate Research Center, and strain 17577 from the Oregon National Primate Research Center (RRV₁₇₅₇₇) (5, 61, 195). As RRV₁₇₅₇₇ was utilized in experiments presented in this dissertation, this strain will be the focus of this section and will be referred to as RRV. Following

sequence analysis of the ~131 kb long unique region of RRV, it was determined that the genome of RRV is co-linear with HHV-8 (Figure 1.6). Specifically, 67 of 79 RRV ORFs are shared with ORFs of HHV-8. In addition, the 53.5% G + C content of RRV is comparable to that of HHV-8 (195). High relatedness is also evident between RRV and HHV-8 when comparing amino acid sequences of six highly conserved viral proteins between gammaherpesviruses (Figure 1.7). Taken together, it was determined that RRV is the rhesus macaque homologue of HHV-8.

b. RRV associated diseases

RRV was isolated from an simian immunodeficiency virus (SIV)-infected rhesus macaque with lymphoproliferative disorder (LPD) (195). It has also been reported that experimental RRV infection of SIV-infected rhesus macaques has led to the development of LPD resembling MCD observed in patients that are co-infected with HIV and HHV-8, further support of the association of RRV with the development of LPD in an immunocompromised host (229). As RRV was recovered from peripheral blood mononuclear cells (PBMCs) of SIV co-infected animals, and RRV gene expression was observed in tissues and PBMCs from these animals, it can be concluded that RRV is associated with development of LPD in these animals (229). In addition, one SIV/RRV co-infected macaque has developed retroperitoneal fibromatosis (RF) (unpublished observation), a vascular neoplasm resembling KS lesions (85). Upon further investigation, RRV was determined to persist in B lymphocytes within an infected host (21). Importantly, despite similar genomic

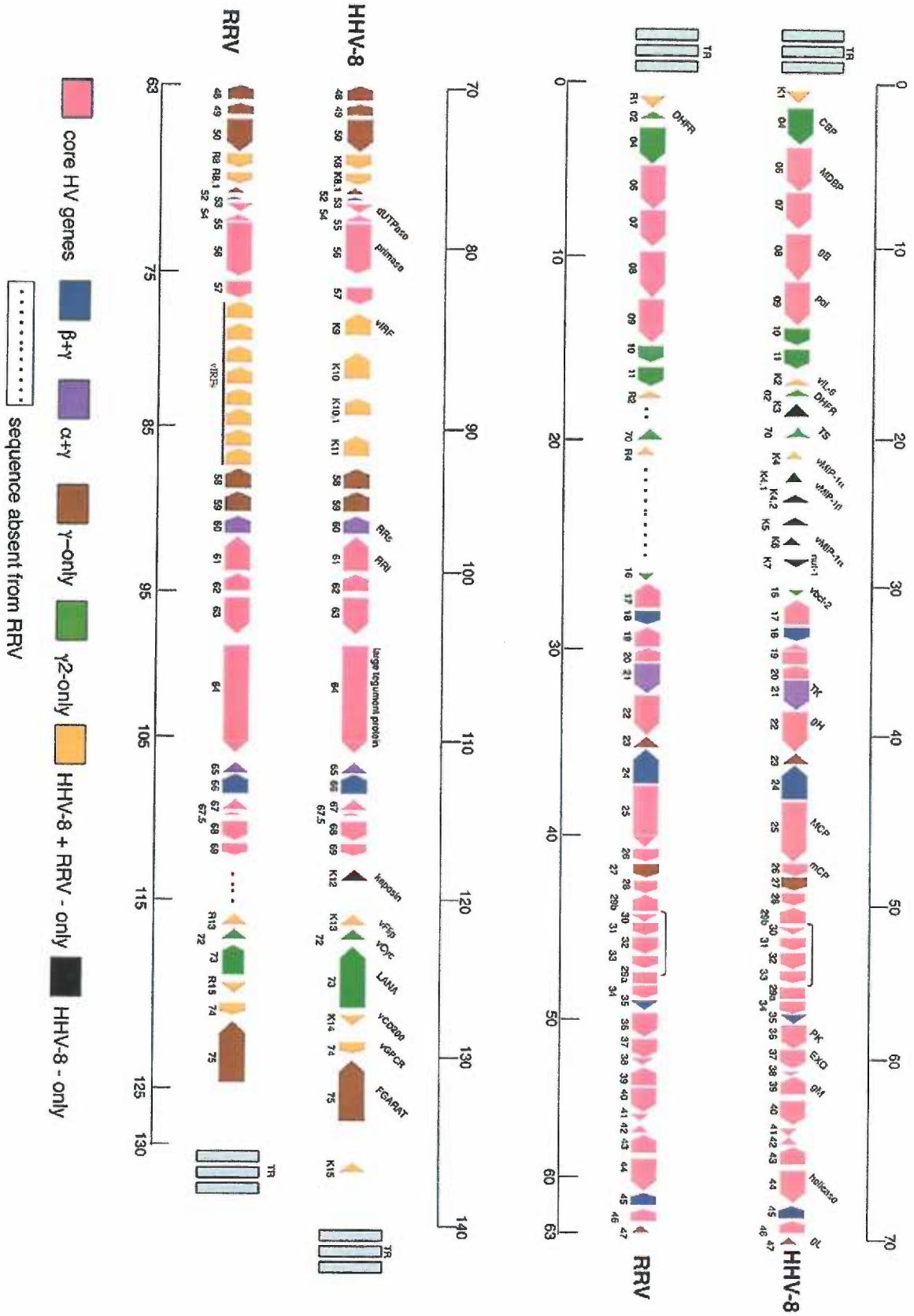
organization and sequence to strain 17577, RRV 26-95 has yet to be associated with disease development in immunosuppressed rhesus macaques.

Sequences from other potential gammaherpesviruses different from RRV have been identified in RF tissue from two macaque species, *Macaca nemestrina* and *Macaca mulatta*. Analysis of RF tissue from these two species of macaques led investigators to believe that a gammaherpesvirus, referred to as retroperitoneal fibromatosis herpesvirus (RFHV), is associated with this disease manifestation (182). While these sequences were identified in 1997, corresponding viruses have not been isolated for further characterization, questioning their authenticity.

c. RRV ORFs associated with pathogenesis

Like HHV-8, many cellular homologues have been identified within the RRV genome, and likely play roles in promoting pathogenesis of RRV. Specifically, RRV encodes a CD200 homologue (vCD200), a viral macrophage inflammatory protein (vMIP), a vIL-6 homologue, a vGPCR, eight viral interferon regulators (vIRFs), a viral cyclin (vCYC) homologue, and apoptotic regulators (vFLIP, vBcl-2) (195). RRV vIL-6 has been characterized and retains IL-6 like activity in that it can support the growth of B cells that are dependent on the presence of this cytokine (109). The function of the vGPCR has also been examined and was found to be similar to the HHV-8 encoded vGPCR. In this study, RRV vGPCR promoted transformation of NIH 3T3 cells and tumorigenesis in a nude mouse model. In addition, RRV vGPCR was also found to induce secretion of VEGF and activation of the mitogen-activated protein kinase signaling pathway (71).

Figure 1.6 Alignment of the genome RRV with the genome of HHV-8. The colors indicate the predicted ORFs contained in HHV-8 and RRV. The terminal repeat (TR) regions are also noted. Numbers on the figure represent kilobases of nucleotide sequence. ORFs are not drawn to scale. *Figure adapted from (5).*



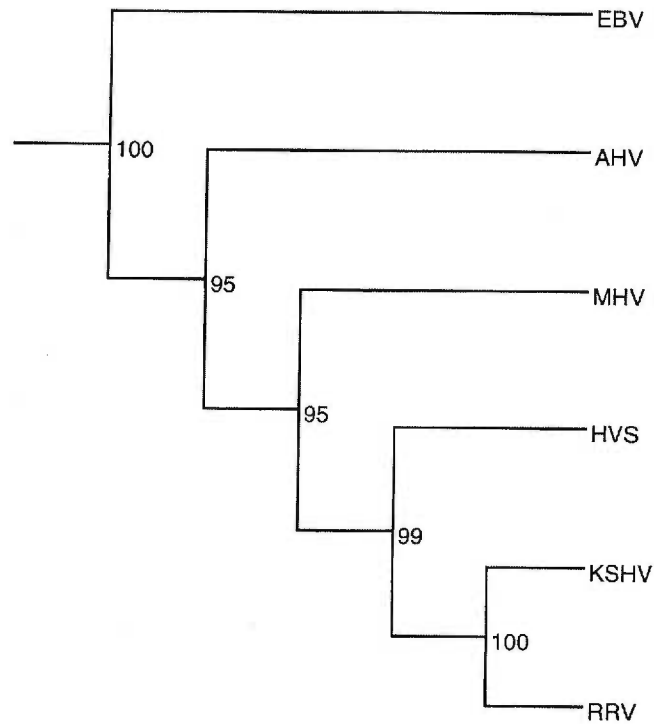


Figure 1.7 Phylogenetic tree of the gammaherpesvirus, indicating high genetic relatedness of RRV with HHV-8. This diagram represents the consensus phylogenetic tree from the analysis of six core viral genes (ssDPB [single stranded DNA binding protein], gB [glycoprotein B], Pol [DNA polymerase], MCP [major capsid protein], Hel [helicase], UDG [uracil-DNA glycosylase]). The numbers represent the number of Protpars trees out of 100 that contained the same sequences to the right of the branch point as in the consensus tree. EBV= Epstein-Barr virus, AHV= alcelaphine herpesvirus, MHV= murine gammaherpesvirus 68, HVS= herpesvirus saimiri, KSHV= Kaposi's sarcoma-associated herpesvirus/human herpesvirus-8, RRV= rhesus rhadinovirus. *Figure and legend adapted from (195).*

d. RRV as a model for HHV-8 infection

To gain further understanding into the mechanisms of HHV-8 pathogenesis and disease progression within an immunocompromised host, an animal model is absolutely necessary. It has been demonstrated that RRV shares genomic co-linearity and a majority of ORFs with HHV-8 (195). This is a distinguishing factor between RRV and MHV-68, given that MHV-68 lacks homologous ORFs likely involved in HHV-8 pathogenesis, including a vCD200 homologue. Further, co-infection of SIV-infected rhesus macaques with RRV has resulted in disease formation closely resembling that observed in HIV/HHV-8 coinfecting individuals (229). Also, the genetic relatedness of the rhesus macaque is much higher than a mouse in comparison to humans, therefore, immunological phenomena related to these infections can be better understood in the non-human primate model. Taken together, these observations strengthen the SIV/RRV co-infected rhesus macaque as a model for HIV/HHV-8 pathogenesis and disease progression in humans.

7. RRV vCD200 as a model for HHV-8 vCD200 pathogenesis

a. Preliminary analysis of RRV R15

Upon initial examination, RRV R15 appears to encode for a viral CD200 homologue. Sequence comparisons of RRV vCD200 with HHV-8 vCD200 and human CD200 reveal that the RRV protein is 30% identical to the human protein and

28% identical to the HHV-8 homologue. While these levels of similarities are not great, the predicted folding pattern of RRV vCD200 appears to match that of the human and HHV-8 proteins (Figure 1.5). In addition, the co-linearity of RRV vCD200 with HHV-8 vCD200 is highly suggestive that these proteins will function similarly. While RRV vCD200 is likely to behave similar to CD200, this needs to be experimentally determined. Any differences between the viral homologues will also need to be identified, as these differences may translate into variabilities in viral pathogenesis. Understanding how this protein contributes to viral pathogenesis is key in utilizing RRV as a model for HHV-8 infection.

b. Overview of thesis project

It is the focus of this dissertation to characterize RRV vCD200 on two levels. First, it is important to determine the kinetic class and characteristics of the R15 transcript during RRV infection. Utilizing the RRV *in vitro* model of infection of primary rhesus fibroblasts, it was determined that the transcript encoding vCD200 is a late-lytic transcript and is bicistronic with ORF74. The R15 transcript is similar to the K14 transcript in that they are both bicistronic with ORF74, however, the kinetic class differs, as the K14/ORF74 transcript appears at an early time point. Further, we have identified a unique splicing event that occurs in the RRV transcript, which removes the transmembrane region of R15, allowing for a truncated version of vCD200 to be produced and secreted from an infected cell. This collection of work describing R15 transcripts is presented in Chapter 2. Secondly, the biological function of vCD200 must be determined. To facilitate these experiments, a soluble form of

vCD200 was generated, fusing the predicted extracellular domain of vCD200 with the Fc portion of human IgG. Human CD200-Fc was also generated and both of these proteins were purified from supernatants of transfected CHO cells. Human THP-1 monocytes were differentiated into macrophages and incubated with Fc fusion proteins to measure the effect of TNF production in comparison to macrophages incubated with Fc alone. It was determined that RRV vCD200-Fc behaves similarly to human CD200 in downmodulating macrophage activation as measured by a reduction in levels of TNF RNA and secreted protein. In addition to human monocyte-derived macrophages, primary rhesus monocyte-derived macrophages secreted a reduced amount of TNF in response to RRV vCD200-Fc. We have also reported that RRV vCD200 is expressed on the surface of primary rhesus fibroblasts during lytic RRV infection. The collection of work to preliminarily characterize and assess the function of RRV vCD200 is presented in Chapter 3.

c. Significance of this work

To assess the viability of RRV as a model for HHV-8 infection, it is necessary to characterize the RRV ORFs that are believed to be involved in promoting viral pathogenesis in HHV-8. Should RRV ORFs contribute to disease progression similarly to those in HHV-8, the RRV model of HHV-8 infection will be strengthened. Here, novel findings of a viral CD200 homologue are presented and further support RRV as a suitable animal model for HHV-8. As CD200 has been associated with promoting a state of immune tolerance, it is conceivable that vCD200

could also be used therapeutically to control myeloid cell activation in transplant systems, allowing for the potential of enhanced organ survival.

d. Author's contributions

In chapter 2, the author of this dissertation contributed 50% effort to each figure (Figures 2.1-2.4). All work presented in chapter 3 was performed by the author

Splicing of rhesus rhadinovirus R15 and ORF74 bi-cistronic transcripts during lytic infection and analysis of effects on production of vCD200 and vGPCR

Carly L. Pratt^{1,3,+}, Ryan D. Estep^{1,3,+} and Scott W. Wong^{1,2,3,*}

Vaccine and Gene Therapy Institute¹, Oregon Health & Science University West Campus, Division of Pathobiology and Immunology², Oregon National Primate Research Center, Beaverton, Oregon 97006;
Department of Molecular Microbiology and Immunology³, Oregon Health & Science University, Portland, Oregon 97201.

⁺ These authors contributed equally to the study.

^{*} Corresponding author:

Vaccine and Gene Therapy Institute
Oregon Health & Science University, West Campus
505 N.W. 185th Avenue
Beaverton, Oregon 97006
Tel: (503)-690-5285
Fax: (503)-418-2719
e-mail: wongs@ohsu.edu

Running title: Transcriptional Analysis of RRV R15 and ORF74

An altered version of this manuscript is published in *Journal of Virology*, March 2005;79:3878-82.

ABSTRACT

Human herpesvirus-8/ Kaposi's sarcoma-associated herpesvirus (HHV-8/KSHV) is the etiological agent of Kaposi's sarcoma (KS), the most predominant AIDS-associated malignancy, as well as lymphoproliferative disorders including multicentric Castleman's disease (MCD), primary effusion lymphoma (PEL), and some non-Hodgkin lymphomas (NHL). The rhesus macaque homologue of HHV-8, rhesus macaque rhadinovirus (RRV), has been associated with lymphoproliferative disease in simian immunodeficiency virus (SIV)-infected macaques, with the primary display of disease being B cell hyperplasia and MCD. Understanding the roles of pathogenic open reading frames (ORFs) in RRV-associated disease is critical to developing RRV as an animal model to study the contributions of individual viral ORFs to HHV-8 pathogenesis. Here we examine the transcriptional pattern of RRV R15 and ORF74. RRV ORF74 is similar to HHV-8 ORF74, encoding a constitutively active and transforming viral G protein-coupled receptor (vGPCR). R15 is highly similar to K14 of HHV-8, which encodes a putative homologue of a cellular immunoregulatory protein CD200. As in HHV-8, the message encoding RRV R15 and ORF74 is bi-cistronic. However, unlike what has been suggested for HHV-8, RRV R15 and ORF74 encoding transcripts are expressed late during lytic infection, and undergo unique splicing events that result in the production of bi-cistronic transcripts capable of encoding vGPCR, as well as membrane-associated and secreted forms of vCD200. This is a novel finding for any CD200 or CD200-like protein, and could have major implications for a role for this protein in virally induced disease.

INTRODUCTION

Rhesus macaque rhadinovirus (RRV) has been demonstrated to be the rhesus macaque homologue of human herpesvirus-8 (HHV-8)/Kaposi's sarcoma-associated herpesvirus (KSHV) (61, 195). HHV-8 is the etiological agent of Kaposi's Sarcoma (KS), the most common AIDS-associated neoplasm, as well as B cell malignancies including primary effusion lymphoma (PEL), multicentric Castleman's disease (MCD), and some non-Hodgkin lymphomas (NHL) (26, 39, 42, 159, 200). Our laboratory has previously identified an independent RRV isolate, termed 17577, from an SIV-infected rhesus macaque which had developed lymphoproliferative disorder (LPD) (195). Sequencing of the complete genome of this RRV isolate provided evidence that, indeed, this virus is highly homologous to HHV-8. In addition, further work done in our laboratory has shown that experimental inoculation of SIV-infected macaques results in these animals developing a lymphoproliferative disorder similar to MCD in AIDS patients infected with HHV-8 (229). Also, experimental infection with RRV₁₇₅₇₇ is potentially associated with the development of retroperitoneal fibromatosis (RF), a disease that displays cellular characteristics similar to KS (unpublished observation). Therefore, the SIV/RRV₁₇₅₇₇ system provides an excellent animal model to study the contributions of RRV to disease manifestations that are similar to those seen with HIV/HHV-8 infection in humans.

Examination of the RRV genome shows that this virus maintains numerous open reading frames (ORFs) that are found in HHV-8. Specifically, 67 of 79 ORFs encoded by RRV are similar to those in HHV-8. Studies to examine the properties of individual ORFs in RRV will help to decipher exactly how similar and/or different

RRV is to HHV-8, and will ultimately determine the importance of the SIV/RRV model to understanding HHV-8 pathogenesis in HIV infected individuals. Thus far, the examination of several ORFs from RRV has demonstrated that they appear to have similar functions and activities to their counterparts in HHV-8. For example, the RRV IL-6 homologue (vIL-6), encoded by ORF R2, has been shown to be a functional IL-6 homologue, similar to vIL-6 of HHV-8 (109). In addition, the RRV G protein-coupled receptor (GPCR), encoded by ORF74, is a seven-transmembrane receptor that displays similar properties to the homologous protein encoded by ORF74 in HHV-8. Like ORF74 of HHV-8, RRV ORF74 has been shown to encode a constitutively signaling GPCR with transforming potential (71). Work has also been done to characterize the R1 protein from RRV, demonstrating similar transforming potential and lymphocyte signaling abilities as the homologous KSHV K1 protein (57, 58), and to identify the RRV bZIP and Rta homologues (133). Another RRV ORF of interest is R15, which to date has not been examined in detail. R15 appears to be homologous to ORF K14 of HHV-8, which encodes a putative viral CD200 (vCD200) homologue similar in sequence and predicted structure to human CD200 (huCD200). Specifically, these proteins are predicted to be type-I transmembrane proteins with two immunoglobulin domains in the extracellular region. It has been shown that engagement of huCD200 with its corresponding receptor (CD200R) on cells of myeloid lineage results in the production of an anti-inflammatory (TH2) cytokine response from these cells (88, 102, 231), while examination of the properties of HHV-8 vCD200 suggest that the extracellular domain of this protein induces an opposite, pro-inflammatory (TH1), cytokine response from cells of myeloid lineage

(50). Despite apparent differences in the activities of these proteins, it appears that both proteins possess immuno-regulatory properties. Thus, the possibility exists that vCD200 proteins may play an important role in the modulation of the host immune response during viral infection.

Transcriptional analysis of various ORFs in HHV-8 has demonstrated that the transcriptional patterns of viral ORFs can be intricate and complicated. For example, analysis of HHV-8 ORF74 has revealed that this ORF is transcribed as the second ORF of bi-cistronic messages with ORF K14, the ORF encoding the viral CD200 homologue. The studies examining the transcription of this region of the HHV-8 genome seem to suggest that both the vCD200 and vGPCR proteins are made in full-length from these bi-cistronic transcripts, however this has not been demonstrated. In addition, detection of the K14 and ORF74 transcripts has been reported to occur early during lytic HHV-8 gene expression (47, 116, 153, 209). To date, transcriptional analysis of RRV ORFs have been limited (62). Here we demonstrate that similar to K14 and ORF74 in HHV-8, RRV R15 and ORF74 are also encoded on bi-cistronic transcripts. However, in the case of RRV, the transcripts encoding these ORFs are made late during RRV lytic infection. In addition, further examination of these RRV transcripts reveals that a unique splicing event occurs within the R15-ORF74 coding sequence that allows RRV vCD200 to be produced as a soluble/secreted protein, a novel finding for a viral CD200-like protein that could have major implications in viral-mediated pathogenesis.

MATERIALS AND METHODS

Cells and virus. Primary rhesus fibroblasts were grown in Dulbecco's modification of Eagle's medium (DMEM) (Mediatech, Herndon, VA) supplemented with 10% fetal bovine serum (HyClone, Logan, UT). Viral stocks used were obtained by infection of primary fibroblasts with RRV₁₇₅₇₇ clone #7. For virus infection studies, cell cultures were grown in either the presence or absence of inhibitors (cycloheximide [75 µg/mL] or phosphonoacetic acid [300 µM]) (Sigma) for two hours and then infected with RRV at a multiplicity of infection (MOI) of 5 in the presence of inhibitors. Chinese hamster ovary (CHO) cells were grown in F12K media (Mediatech) containing 5% fetal bovine serum (HyClone). Nucleotide sequence accession number for RRV₁₇₅₇₇ is AF083501.

RNA. Total RNA was obtained from primary rhesus fibroblasts cultures infected with RRV using TRI Reagent (Sigma, St. Louis, MO) according to manufacturer's specifications. RNA used in RT-PCR from transfected CHO cells was isolated using Hi Pure RNA Isolation Kit (Roche, Nutley, NJ) per manufacturer's instructions.

Northern Blot analysis. RNA was run on 1.0% agarose gels containing 1.0% formaldehyde, with 10 µg of total RNA loaded per lane. Gels were then transferred to nitrocellulose membranes, and probed with specific dsDNA or oligo probes using standard protocols. dsDNA probes were generated by random primed labeling with specific cloned DNA fragments for the entire R15 or ORF74 sequence, using

[α -³²P]dCTP and a random prime labeling kit (Stratagene, La Jolla, CA). R15 oligo probe (5'-GGTCGTTCTGGTCAACTTGTGTTC-3') and ORF73 oligo probe (5'-TTCCCATAACCGTATCCCTCATCAG-3') were generated by end-labeling oligos with [γ -³²P]ATP using polynucleotide kinase (Fermentas, Hanover, MD). As loading control, blots were stripped using 0.1% boiling SDS, and re-probed with a [α -³²P]dCTP labeled dsDNA probe specific for rhesus GAPDH.

Reverse Transcription-PCR (RT-PCR) of spliced transcripts. RT-PCR was performed using a Titan One-step RT-PCR kit (Roche), following manufacturer's instructions. 500 ng of RNA was used per reaction, utilizing conditions that were optimized for each specific reaction. Reactions containing Vent DNA polymerase without RT enzyme served as controls to demonstrate the absence of DNA. Primers used to amplify the upstream region of the R15-ORF74 transcript were specific for ORF71 (5' primer: 5'-ATCGCCCAACGAGAAACA-3') and R15 (3' primer: 5'-AATGTAAATCCTCCCGACAT-3'), while those used to amplify the R15-ORF74 region were specific for R15 (5' primer: 5'-ATGTCGGGAGGAA-3') and ORF74 (3' primer: 5'-TCATAAACTACCTGAAGTGGA-3'). Products were analyzed on 1.7% agarose gels, then purified and cloned into pCRII-Topo vector for sequencing.

Protein expression analysis of spliced transcripts. An internal FLAG epitope tag was introduced to R15 coding sequence (at nt 632) by PCR using a R15 specific primer containing the FLAG sequence as the 3' primer (5'-GCCGCGGCCTTGTCGTCGTCGTCCTTGTAATCCAAACCGCCTATATGAGT-

3'), a primer for the exact 5' end of R15 sequence, and 2.1 kb R15-ORF74 cDNA as template. PCR products were then cloned into 1.7 kb and 2.1 kb R15-ORF74 cDNAs from RT-PCR using a unique *Sac*II site located within R15 sequence. The FLAG coding sequence of these constructs is in frame with vCD200 protein, and is located upstream of the splice site identified in this region. A C-terminal HA epitope was introduced in frame with vGPCR by performing PCR with either the 1.7 kb or 2.1 kb R15-ORF74 cDNAs as templates, using a 5' R15 primer and a 3' ORF74-HA primer (5'-
TCAAGCGTAGTCTGGGACGTCGTATGGGTATAAACTACCTGAAGTGGAA-
3'). Epitope sequences are underlined. All products were sequenced to confirm their identity and cloned into pcDNA3.1(-) (Invitrogen) for expression analysis. For immunofluorescence analysis, CHO cells were plated the day before transfection on chamber slides (Nunc, Naperville, IL), and transfected using Transit LT-1 reagent (Mirus, Madison, WI) with 0.5 µg of DNA per chamber. Approximately 48 hours post-transfection, cells were fixed with 100% cold methanol, stained for FLAG or HA using the appropriate primary antibodies (Sigma), and a FITC-labeled secondary antibody (Sigma). Fixed cells were then analyzed by confocal microscopy using a TCS SP confocal system (Leica Microsystems, Heidelberg, Germany) with a Plan Apo 40X or 100X objective. FACS analysis was performed on live CHO cells 48 hours post-transfection following staining with FLAG specific antibodies (FACSCalibur, Becton Dickinson, San Jose, CA). For Western blot analysis of vCD200-FLAG expression, CHO cells were plated in 6-well dishes the day before transfection, and were transfected with either empty vector, 1.7 kb R15-FLAG, or 2.1

kb R15-FLAG, using Transit LT-1 reagent with 3 μ g DNA per well. Supernatants were then collected at 48 hours post-transfection and concentrated using Amicon ultra centrifugal filter devices (Millipore, Bedford, MA). Lysates from these same cells were prepared by lysing cells in RIPA buffer (1X PBS + 1% NP-40, 0.1% SDS, 0.5% sodium deoxycholate). 50 μ l of concentrated supernatant, and 50 μ l of lysates were run on 10% acrylamide gels, transferred to nitrocellulose membranes, and probed with anti-FLAG antibody. To detect HA tagged ORF74 protein, CHO cells were plated in 60 mm dishes the day before transfection, and then transfected with either empty vector, 1.7 kb ORF74-HA, 2.1 kb ORF74-HA, or pcDNA3.1(-) encoding an N-terminally tagged version of RRV ORF74 as a control. Cells were lysed 48 hrs post-transfection with 500 μ l RIPA per dish, and HA tagged protein was immunoprecipitated by incubating lysates overnight with anti-HA antibody (Sigma) and protein A beads. The beads were then washed 4X with PBS, and immunoprecipitated protein was then eluted by incubation with 2X SDS-PAGE buffer at 37°C for 1 hr before loading onto a 10% acrylamide gel. The gel was transferred to a nitrocellulose membrane and probed with anti-HA antibody (Sigma).

Prediction of protein signal sequence. The program SignalP was utilized to predict signal sequences within RRV vCD200 (158).

RESULTS

Northern Blot Analysis of R15 and ORF74 transcripts. Figure 2.1A depicts the region of the RRV genome encoding R15 and ORF74. To examine the expression pattern of RRV R15 and ORF74, we utilized our *in vitro* system of RRV infection of primary rhesus fibroblasts to obtain total RNA from infected cells. Primary rhesus fibroblasts were infected with RRV₁₇₅₇₇ in the presence of cycloheximide (CHX) to inhibit protein synthesis, phosphonoacetic acid (PAA) to inhibit DNA replication, or left untreated to detect immediate-early, early, or late viral transcripts, respectively. The time points for collection of RNA were 24 hours (CHX), 48 hours (PAA), and 72 hours (untreated), as these three classes of transcripts have been determined to roughly appear at these time points after infection with RRV *in vitro*, even in the absence of inhibitory drugs. As seen in Figure 2.1B and C, both ORF74 and R15 transcripts are only detected in untreated cultures collected 72 hrs post-infection, demonstrating that these ORFs are transcribed as late-lytic genes.

Examination of the RRV transcripts seen by Northern blot analyses indicate that the similar size species of transcripts are detected using either a double-stranded R15 or ORF74 DNA probe, suggesting that as in HHV-8, these two ORFs could in fact be encoded together on bi-cistronic messages. Interestingly, there appears to be at least two RNA species present encoding R15 and ORF74, a large transcript of approximately 5.5 kb and a smaller transcript of approximately 3.0 kb. The presence of other transcripts is also possible, since the bands in the Northern blots are somewhat diffuse in both cases. One possible explanation for the larger transcript is that it represents an antisense message that is transcribed from the opposite strand of

the viral genome, initiating somewhere near the right end (3') of ORF74 and extending through both ORFs. If this were true, this message would be detectable when using double-stranded DNA (dsDNA) probes, but not with an anti-sense oligo probe. To examine this possibility, we used an antisense oligo probe specific for R15 in Northern analysis of 72 hr/untreated RNA. Using this probe we were able to detect two messages of similar size to those obtained when using the dsDNA probes for R15 and ORF74 (Fig. 2.1D), suggesting that the two bands seen in Northern analysis are indeed specific for transcripts initiating in a region upstream of R15 and extending through ORF74. In addition, bands for any apparent mono-cistronic R15 or ORF74 messages were not detected in Northern analyses.

RT-PCR analysis of R15-ORF74 bi-cistronic message. Northern blot analyses suggest that R15 and ORF74 are co-transcribed on the same message. Therefore, we sought to confirm this by RT-PCR analysis. This approach would also allow us to determine if this transcript was spliced in the region encoding both ORFs, as is the case of HHV-8 K14 and ORF74, in which 149 bp between the two ORFs is spliced from the K14-ORF74 containing transcript (47, 116, 153, 209). We designed primers to bind at the exact 5' end of R15 sequence and the exact 3' end of ORF74 sequence to amplify the corresponding message from RNA obtained from RRV-infected primary rhesus fibroblasts. The expected size for this product would be 2.1 kb for an unspliced message containing both ORFs, while anything smaller than this size would represent potential spliced message(s). Using 72 hr/untreated RNA in this analysis, we amplified two predominant products. Specifically, we detected a 2.1 kb product

likely representing the entire unspliced region, and a more abundant 1.7 kb product, indicating that splicing of the 2.1 kb message is taking place (Fig. 2.2A). No products were detected in control reactions containing no RT enzyme. The finding that the 1.7 kb product is in greater abundance compared to the 2.1 kb product suggests that this spliced message may be the predominant form of the transcript found in RRV-infected cells undergoing lytic replication.

To identify the sequence of the spliced message, and confirm the identity of the unspliced message, we isolated both products obtained by RT-PCR and sequenced five cDNA clones of each. The sequences of all 2.1 kb cDNA clones were identical, and confirmed the identity of the full-length, and therefore unspliced, R15 and ORF74 region of the bi-cistronic transcripts. Sequences from the cDNA clones corresponding to the more abundant 1.7 kb species were all identical, and demonstrated the presence of a splice donor at nt 123555 (within R15 sequence) and a splice acceptor at nt 123916 (8 nt upstream of the ORF74 ATG) (Fig. 2.2C). The donor sequence motif (*G'GTGGGT*) is identical to the donor sequence identified in the splice of K14 and ORF74 in HHV-8, while the acceptor motif (*TGTCAG'A*) is more divergent from the motif found in HHV-8 (*TTGTAG'G*) (47, 116, 153, 209). Unlike what has been reported for HHV-8, in which neither K14 or ORF74 coding sequence is altered, the splice event in the RRV transcript removes 72 bp from the 3' end of R15 coding sequence, making the stop codon for this shortened form of R15 a TGA located 8 bp downstream of the ATG for ORF74 (Fig. 2.2C). This splice would therefore affect the predicted vCD200 expression pattern of the transcript, creating an altered form of vCD200 with 24 aa deleted from the C terminus (amino acids 230-

254), and a series of 6 new amino acids in its place (TTTWTP). Importantly, the 24 aa region deleted from vCD200 contains the predicted transmembrane domain of this protein (amino acids 229-250), suggesting there may be a soluble form of vCD200 expressed during lytic replication (Fig. 2.2D).

Examination of expression patterns of R15 and ORF74 from spliced and unspliced bi-cistronic messages. First, we wanted to test the ability of cellular machinery to splice transcripts generated from the 2.1 kb R15-ORF74 cDNA. CHO cells were transfected with an expression vector containing the 2.1 kb R15-ORF74 cDNA or empty vector, and RNA was isolated at 48 hrs post-transfection. RT-PCR was then performed with a 5' R15-specific primer and a 3' ORF74-specific primer. Interestingly, both species of R15-ORF74 bi-cistronic transcripts (2.1 kb and 1.7 kb) were present within these cells (data not shown). CHO cells transfected with empty vector did not test positive for either transcript. Therefore, in cells transfected with the full-length/unspliced 2.1 kb R15-ORF74 cDNA expressing vector, both spliced and unspliced versions of the R15-ORF74 message are present.

After discovering that R15 and ORF74 are encoded on the same bi-cistronic late-lytic messages, and that these transcripts contain a splice site between the two ORFs, we next wanted to examine the protein expression patterns from transcripts that have been spliced or remain unspliced in this region. To facilitate expression analyses without antibodies to these viral proteins, we performed PCR using a sequenced R15-ORF74 cDNA clone of each transcript variant as a template (spliced/1.7 kb or unspliced/2.1 kb), to introduce an internal FLAG-epitope tag in

frame with vCD200, and to introduce an HA-epitope tag to the C-terminus of vGPCR. To avoid disruption of the predicted N-terminal signal sequence of RRV vCD200 (158), a FLAG tag was introduced upstream of the identified splice site at nt 632 of R15. The internal FLAG-tagged R15 constructs were named 1.7 kb R15-FLAG and 2.1 kb R15-FLAG, while the C-terminal HA tagged ORF74 constructs were named 1.7 kb ORF74-HA and 2.1 kb ORF74-HA.

To initially assess the expression from these constructs, CHO cells were transiently transfected with empty vector, 1.7 kb R15-FLAG, 1.7 kb ORF74-HA, 2.1kb R15-FLAG, or 2.1 kb ORF74-HA. Approximately 48 hr post-transfection, these cells were stained with antibodies specific for the FLAG or HA epitopes and examined by immunofluorescent confocal microscopy. Cells transfected with the full-length 2.1 kb R15-FLAG showed specific staining, with the cellular distribution of vCD200-FLAG appearing mostly cytosolic, with some areas of apparent membrane staining (Fig. 2.3A). A similar staining pattern was observed with cells transfected with 2.1 kb ORF74-HA (Fig. 2.3B), demonstrating that vCD200 and vGPCR proteins are both made from this full-length species of transcript. To our knowledge, this demonstrates for the first time that a viral GPCR can be expressed as the second ORF on a bi-cistronic transcript.

When examining staining of cells expressing the spliced 1.7 kb R15-FLAG transcript, we found that the vCD200 staining was generally cytosolic, and importantly, absent from the plasma membrane (Fig. 2.3C). The pattern of vCD200 expression from the 1.7 kb R15-FLAG vector suggests that the truncated version of vCD200 expressed from the spliced transcript is no longer localized to the plasma

membrane, the predicted outcome of deleting the RNA sequence encoding the putative transmembrane region of the protein. vGPCR staining is also detected in the cytoplasm and on the surface of cells transfected with the 1.7 kb R15-ORF74 cDNA (Fig. 2.3D). Therefore, splicing of the 2.1 kb R15-ORF74 transcript does not abrogate vGPCR expression.

To further demonstrate that the transmembrane region is necessary for cell surface expression of vCD200, live transiently transfected CHO cells were stained for surface expressed vCD200 with anti-FLAG antibody and subjected to FACS analysis. When compared to vector-transfected cells, cells expressing vCD200 from the 1.7 kb R15-FLAG construct demonstrated very low levels of surface staining (2.24%), while cells transfected with the 2.1 kb R15-FLAG construct demonstrated significant levels of surface staining (33.4%), confirming that full-length/membrane-associated vCD200 is strictly expressed from the unspliced 2.1 kb R15-ORF74 transcript (Fig. 2.3E). FACS analysis of fixed/permeabilized cells expressing either the 1.7 or 2.1 kb R15-FLAG constructs indicated equal levels of total vCD200 expression from both constructs (data not shown).

Next, we wanted to determine if vCD200 was indeed capable of being secreted from cells expressing the spliced 1.7 kb or 2.1 kb cDNAs. Western blot analysis of lysates from transiently transfected CHO cells demonstrated that a band of approximately 40 kDa for vCD200-FLAG is detected in cells expressing either 1.7 kb or 2.1 kb R15-FLAG, but not in cells transfected with vector alone (Fig. 2.4B). The predicted size of full-length vCD200-FLAG is 28 kDa, however, the protein has several potential glycosylation sites, which likely accounts for the discrepancy in the

size and the diffuse property of the protein detected by Western blot. Also, since the splicing event that removes the transmembrane region of vCD200 deletes a total of 18 aa residues of protein sequence, both the full-length and spliced species of vCD200 are likely represented by the same approximately 40 kDa band in cells transfected with 2.1 kb R15-FLAG construct. To determine whether a soluble version of vCD200 was being secreted from cells expressing spliced 1.7 kb R15-ORF74 cDNA, supernatants from transiently transfected CHO cells were collected and concentrated for Western blot analysis. As predicted, supernatants from cells transfected with vectors expressing either 1.7 kb or 2.1 kb R15-FLAG contained significant amounts of vCD200 protein, indicating that the 1.7 kb cDNA is indeed capable of producing soluble/secreted vCD200 protein (Fig. 2.4C).

We also sought to confirm the expression of full-length vGPCR from both the 1.7 kb and 2.1 kb cDNAs. Thus, vGPCR expression from either the 1.7 kb or 2.1 kb ORF74-HA constructs was examined by immunoprecipitation of HA tagged protein from transiently transfected CHO cells, followed by Western blot analysis. Detection of a band for the predicted size of the RRV vGPCR in cells transfected with either 1.7 kb or 2.1 kb ORF74-HA constructs demonstrates that full-length protein is capable of being produced from either spliced or unspliced cDNAs (Fig. 2.4A), and suggests that translation of ORF74 still occurs even after splicing has taken place in the region upstream of ORF74 sequence.

DISCUSSION

HHV-8 is the accepted etiological agent of human malignancies including KS, MCD, PEL, and some NHLs. Prior to highly active antiretroviral therapy, KS lesions were the most common disease manifestation observed in AIDS patients, while MCD and PEL are more rare forms of lymphoproliferative disease caused by HHV-8. To understand the pathogenesis of this virus, we utilize rhesus macaque rhadinovirus (RRV), the rhesus macaque homologue of HHV-8, to infect SIV-infected monkeys as a model for HIV/HHV-8 infection. Understanding differences and similarities between these two viruses is critical in continued development of the RRV/rhesus macaque animal model, and for development of potential treatments for HHV-8 associated diseases.

In this study, we have examined transcription from two viral ORFs encoded by RRV, R15 and ORF74, whose homologues in HHV-8 have been postulated to be involved in the development of viral-mediated disease. In studies of the transcription of these ORFs in HHV-8, it was determined that both ORFs are encoded on bi-cistronic messages, and that these transcripts are expressed as early-lytic genes. Although both proteins encoded by these HHV-8 ORFs are believed to be expressed from this bi-cistronic message, the actual protein expression pattern from the HHV-8 transcripts has never been examined. Comparing transcriptional patterns of ORFs shared between RRV and HHV-8 can lend insight into whether or not the products of these ORFs indeed play a similar role during viral infection and disease development.

Northern blot and RT-PCR analyses revealed that RRV R15 and ORF74 are transcribed as bi-cistronic messages, similar to HHV-8 K14/ORF74. However, unlike

the early-lytic expression pattern of HHV-8 K14 and ORF74, RRV R15 and ORF74 are transcribed as late-lytic genes. Although true differences could exist in the patterns of transcription of these genes between HHV-8 and RRV, we believe the discrepancies seen in relation to the assignment of classes of lytic transcripts between these viruses are more likely due to differences in the systems used to analyze lytic transcription by these viruses. Specifically, all of the studies done to date analyzing K14 and ORF74 transcription in HHV-8 have utilized latently-infected B cells induced to undergo lytic replication using phorbol esters, such as 12-*o*-tetradecanoylphorbol-13-acetate (TPA) or *n*-butyrate (47, 116, 153, 209). In these cultures, a small percentage of latently HHV-8-infected cells spontaneously undergo lytic reactivation (~1-2%), even in the absence of drug induction. Therefore, lytic transcripts may already be present to some extent in these cultures even before induction, which could complicate the definitive assignment of a transcript to a particular class of lytic transcript. On the other hand, RRV infection in our *in vitro* system is strictly lytic, allowing for tight regulation of viral gene expression after infection, and eliminating the background of latent gene transcription. Taken together, the RRV system is more accurate when making the assignment of viral genes to a particular lytic class.

Further examination of the transcriptional splicing pattern within the R15 and ORF74 coding sequence by RT-PCR revealed that a splicing event removes 360 bp of sequence in the R15-ORF74 region. Due to the relatively small size of the splice event in the R15-ORF74 region, distinguishing between the different forms of spliced message is not possible by Northern blot analysis, but may account for the diffuse

nature of the bands we detected in our studies. Upon examination of the sequence removed by the splicing event in the R15-ORF74 region, we found that the splice alters the coding capabilities of R15, deleting the coding sequence for the putative transmembrane domain of vCD200. Thus, R15-ORF74 transcripts containing this splice have the potential to encode a soluble form of vCD200, and expression data (IFA, FACS, and Western blot) support this hypothesis. This is a novel finding for any CD200 or viral CD200 homologue. Western blot analysis and immunofluorescence data also demonstrated that full-length vGPCR is translated from spliced and unspliced R15-ORF74 transcript species. This suggests that the splice removed from the region directly upstream of ORF74 does not abrogate expression pattern of the vGPCR. Translation of RRV ORF74 from these bi-cistronic transcripts could be occurring through an internal ribosomal entry site (IRES)-mediated mechanism, or by other mechanisms such as ribosomal scanning, or translational re-initiation, ideas which have also been suggested to be involved in initiation of HHV-8 ORF74 translation (116, 209). Importantly, the finding that RRV vGPCR is in fact expressed from different spliced forms of bi-cistronic transcripts is intriguing, and to our knowledge demonstrates for the first time that a viral GPCR protein is capable of being expressed as the 3' ORF on a bi-cistronic message. The exact importance of the bi-cistronic expression pattern of the vCD200 and vGPCR proteins in RRV and HHV-8 is yet to be determined. However, the tightly linked expression of these proteins in both viruses would suggest an essential function, either directly or indirectly, or perhaps some interplay between the activities that each protein regulates that may be critical to some aspect of the viral life cycle.

The presence of soluble RRV vCD200 during RRV infection could have major implications in altering the function of the immune system of an infected host. The RRV vCD200 protein is similar in sequence to human CD200 (huCD200), and to HHV-8 vCD200, but its function has yet to be understood. huCD200 has been demonstrated to play important roles in controlling the inflammatory response induced by cells of myeloid lineage. Specifically, engagement of the CD200 receptor on cells of myeloid-lineage induces these cells to produce an anti-inflammatory (TH2) response (88, 102, 231), while vCD200 encoded by HHV-8 K14 elicits a pro-inflammatory (TH1) response from these cells, a function exactly opposite of huCD200 (50). Whether the RRV vCD200 protein behaves as an anti-inflammatory or pro-inflammatory protein, the implications that the presence of a soluble CD200 homologue may have during viral infection are substantial, especially in its potential contributions to virus-induced disease. Studies investigating the function of RRV vCD200 are currently underway.

ACKNOWLEDGEMENTS

This work was supported by NIH grants AI07472 (R.D.E.), RR00163 (S.W.W.) and CA75922 (S.W.W.). We thank Dr. Anda Cornea for assistance with confocal microscopy.

Figure 2.1. Northern blot analysis of RRV R15 and ORF74 transcripts. (A) The region in the RRV genome containing ORFs R15 (vCD200) and ORF74 (vGPCR) is shown. The region is located at the extreme right end of the RRV genome. Viral nucleotide numbers are noted and ORFs are drawn to scale. (B-D) RNA from RRV-infected rhesus fibroblasts treated with cycloheximide (CHX), phosphonoacetic acid (PAA), or untreated cultures was collected at 24 hrs, 48 hrs, and 72 hrs post-infection, respectively. Approximately 10 μ g of total RNA was run on denaturing agarose gels, and transferred to nitrocellulose for hybridization to dsDNA probe for ORF74 (B), dsDNA probe for R15 (C), and an oligonucleotide probe for R15 (D). A rhesus GAPDH probe was utilized to demonstrate equal amounts of RNA for each lane in B and C.

A.



B.



C.



D.

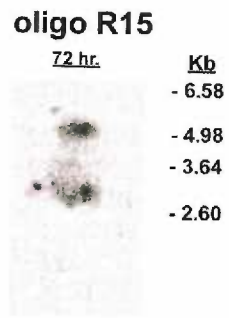
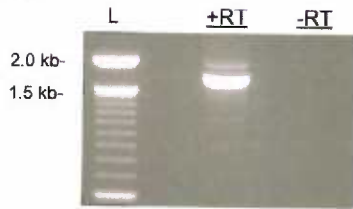


Figure 2.2. Analysis of the splicing pattern within the bi-cistronic R15-ORF74 transcript. (A) Agarose gel of RT-PCR products obtained using 72 hr/untreated RNA with 5' R15 and 3' ORF74 primers. Two bands are detected, one unspliced (2.1 kb), and the other representing a spliced transcript (1.7 kb). (B) Depiction of the R15-ORF74 region, and the predicted splicing pattern based on RT-PCR. (C) DNA sequence alignment of portions of unspliced (2.1 kb) and spliced (1.7 kb) RT-PCR products. Dashes represent region spliced from 1.7 kb message, stop codons for R15 are in gray and the start codons for ORF74 are in black. Note that the stop codon for the spliced R15 sequence is within ORF74 sequence, but in a different reading frame. (D) Diagram of splicing of the bi-cistronic R15-ORF74 transcript. The unspliced transcript loses 360 bp of sequence during splicing, resulting in removal of the coding sequence for the predicted vCD200 transmembrane domain, and generating a transcript potentially encoding a soluble form of vCD200.

A.



B.



C.

```

2.1kb RT-PCR 801 TGCCTGGTCACTCATATAGCCGGTTTGGCCGCGCGCGGCCCTGGACCCCGTGTTCGGATCCCTGGAAAGGACGAGCCACTACGTGGTGGTGTGG 700
1.7kb RT-PCR 801 TGCCTGGTCACTCATATAGCCGGTTTGGCCGCGCGCGGCCCTGGACCCCGTGTTCGGATCCCTGGAAAGGACGAGCCACTACGTTG-----590

2.1kb RT-PCR 751 TGGCAAGGGCCGCGCTTTTAAAGCAATTTTAAACGGGTGTTTTTTGTATAGGTCTATGTGGCCGCGCGTGTCCCGCGTCTAGTGTTTTGTCCCCAG 800
1.7kb RT-PCR 681 -----590

2.1kb RT-PCR 801 TGAATGTCTCCATGACAAATACAAATTTGAGGCTGGCTTTTAAAGGTGTTTCCTTGTGCGACGCTTCTGTGTAACTGCATACACCAGGCGTGTCCGCCAGG 900
1.7kb RT-PCR 691 -----590

2.1kb RT-PCR 901 AAACCGCGTCTCCCTTTATGTCCGCTGCGCCCTCCAGAGCGAAGTGAAGATGTTCCGTGAGGCGTTTTTGGCGTTGAGAGAGTCGGGCGATGTTGCCGT 1000
1.7kb RT-PCR 681 -----590

2.1kb RT-PCR 1001 AGCGGCGTCTGCAAAAGGCTCACCGGCTCTGTTTTTCTTTTGTTCAGACAACAACCTGGAGCCCTTGAACAATAACCTTAACTGCTGATGGATTTT 1100
1.7kb RT-PCR 681 -----590
ACAGGACCTGGAGCCCTTGGACAAATAACCTTAACTGCTGATGGATTTT 740

2.1kb RT-PCR 1101 CTGTCTAACTATTGAAATAGCTACAATAGTTATGACCAAAATATGTCTTACACCTTAGACACCGAATCCAGCGTGTGTGGCGTGAAGGTGTTTTCCAC 1200
1.7kb RT-PCR 741 CTGTCTAACTATTGAAATAGCTACAATAGTTATGACCAAAATATGTCTTACACCTTAGACACCGAATCCAGCGTGTGTGGCGTGAAGGTGTTTTCCAC 840
  
```

D.

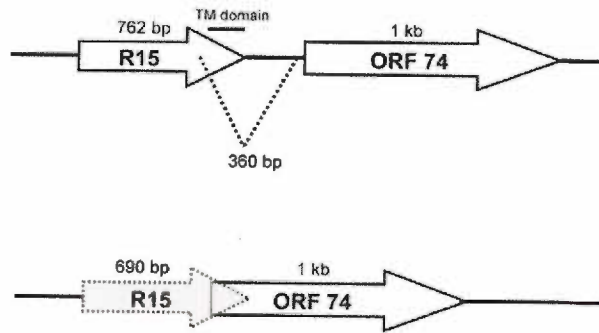


Figure 2.3. Immunofluorescent confocal microscopy and fluorescence activated cell sorting (FACS) analysis of CHO cells transiently expressing 1.7 kb or 2.1 kb bicistronic R15-ORF74 cDNAs. vCD200 contains an internal FLAG epitope tag, while vGPCR contains a C-terminal HA epitope tag. Immunofluorescence analysis (A-D) demonstrates that vCD200 expressed from the 2.1 kb cDNA (A) is detected throughout the cytoplasm and at the cell surface (\wedge), while vCD200 expressed from the 1.7 kb cDNA (C) only displays a cytoplasmic staining pattern. The staining pattern for vGPCR is similar for the 2.1 kb (B) and 1.7 kb (D) versions of cDNA, with protein detected throughout the cytoplasm, as well as at the cell surface. The field shown in panels A, C and D is 512 x 512 microns, panel B is 1024 x 1024 microns. (E) Live cells were stained for FLAG (vCD200) expression and analyzed by FACS. Compared to vector control cells, cells transfected with the 1.7 kb R15-ORF74 cDNA display low levels of surface staining, while cells transfected with the 2.1 kb R15-ORF74 cDNA show significant levels of surface staining, confirming that only the 2.1 kb cDNA is capable of expressing a membrane-associated form of vCD200.

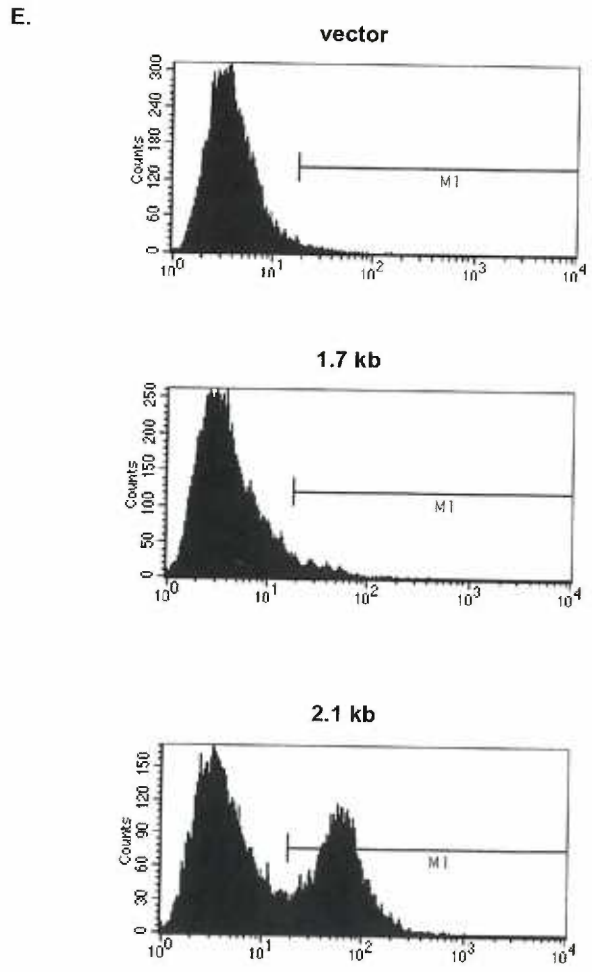
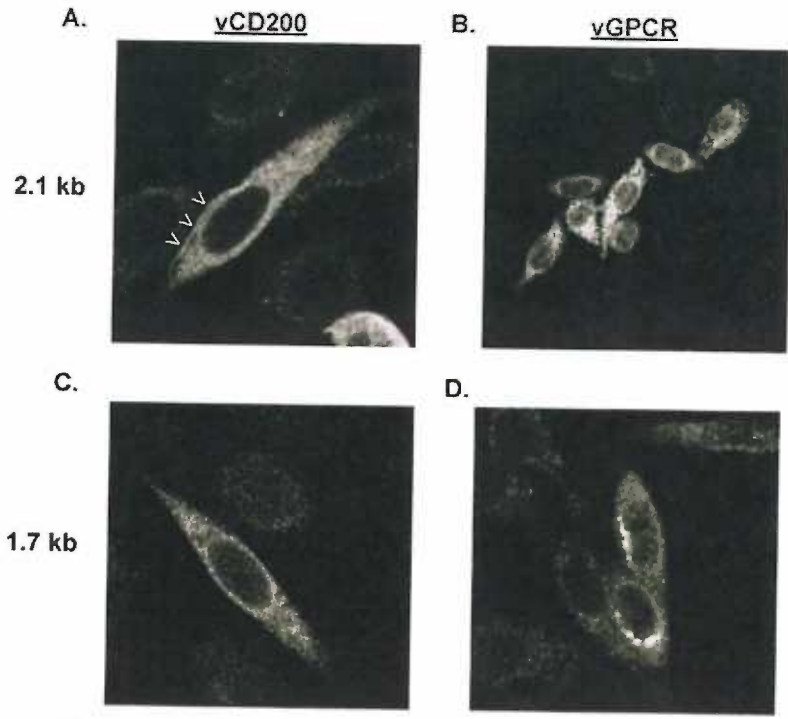
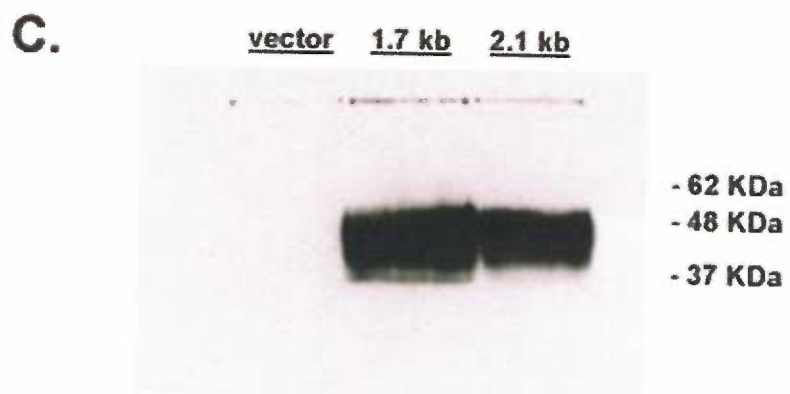
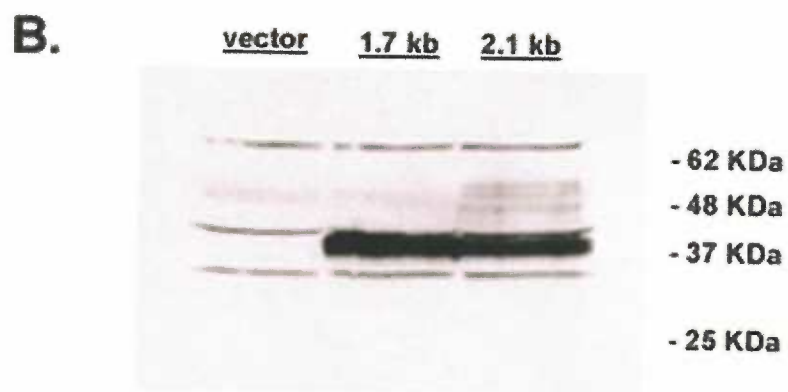


Figure 2.4. Western blot analysis of vCD200 and vGPCR expression. (A) Anti-HA Western of immunoprecipitated lysates from CHO cells transfected with empty vector, 1.7 kb ORF74-HA, 2.1 kb ORF74-HA, or HA-ORF74 expressing control vector. Total cell lysates (B) or concentrated supernatants (C) from CHO cells transfected with empty vector, 1.7 kb R15-FLAG, or 2.1 kb R15-FLAG were analyzed for recombinant vCD200-FLAG expression.



Chapter 3

Rhesus rhadinovirus R15 encodes a functional homologue of human CD200

Carly L. Langlais^{1,3} and Scott W. Wong^{1,2,3,*}

Vaccine and Gene Therapy Institute¹, Oregon Health & Science University West Campus, Division of Pathobiology and Immunology², Oregon National Primate Research Center, Beaverton, Oregon 97006; Department of Molecular Microbiology and Immunology³, Oregon Health & Science University, Portland, Oregon 97201.

* Corresponding author:

Vaccine and Gene Therapy Institute
Oregon Health & Science University
West Campus
505 N.W. 185th Avenue
Beaverton, Oregon 97006
Tel: (503)-690-5285
Fax: (503)-418-2719
e-mail: wongs@ohsu.edu

Running title: Characterization of RRV vCD200

Manuscript was submitted to the *Journal of Virology* on August 12, 2005

ABSTRACT

Through evolution with their host, herpesviruses have pirated cellular genes to aid in the establishment of virus infection and persistence. For example, many immune modulatory genes have been incorporated into viral genomes and these promote viral fitness during infection. Among the pirated immune modulatory genes are those encoding homologues of cellular CD200. Here, we describe a viral CD200 homologue (vCD200) encoded by the simian herpesvirus rhesus rhadinovirus (RRV), the rhesus macaque homologue of human herpesvirus-8 (HHV-8). RRV vCD200, encoded by ORF R15, is similar in structure to and shares 30% amino acid identity with human CD200, and 28% identity with HHV-8 vCD200. To facilitate purification of vCD200, a fusion protein was generated in which the Fc portion of human IgG₁ was fused to the predicted extracellular domain of vCD200. Purified vCD200-Fc is expressed from CHO cells as a glycoprotein with a core molecular weight of ~53 kDa. Immunofluorescence assays with a monoclonal antibody specific for vCD200 revealed vCD200 expression on the surface of RRV-infected fibroblasts. Further, data from *in vitro* assays demonstrated that recombinant vCD200-Fc was found to down modulate TNF expression at the transcriptional level and at the protein level from activated human monocyte-derived macrophages. Primary rhesus macrophages responded similarly to vCD200-Fc treatment in that the levels of TNF detected in treated cell supernatants were reduced compared to controls. These results indicate that RRV encodes a functional homologue of cellular CD200 and that the viral protein could aid in the establishment of a persistence viral infection by down regulating the host innate immune response.

INTRODUCTION

Human herpesvirus-8/Kaposi's sarcoma-associated herpesvirus (HHV-8/KSHV) has been associated with development of Kaposi's sarcoma (KS) lesions (20, 175), multicentric Castleman's disease (MCD) (160, 200) and primary effusion lymphoma (PEL) (36, 82, 84, 112, 152, 153, 163) in AIDS patients. To understand the contributions of HHV-8 to the establishment and progression of these diseases, an animal model of HHV-8 infection within an immunocompromised host is desirable. A rhesus macaque homologue of HHV-8, rhesus macaque rhadinovirus strain 17577 (RRV₁₇₅₇₇), was isolated from a simian immunodeficiency virus (SIV)-infected rhesus macaque displaying lymphoproliferative disease. Sequence analysis of RRV has revealed high relatedness to HHV-8, as these two genomes are co-linear, and 67 of 79 RRV open reading frames (ORFs) are similar to those in HHV-8 (195). More importantly, experimental infection of SIV-infected rhesus macaques with RRV₁₇₅₇₇ results in B cell hyperplasia and disease resembling MCD that is observed in HHV-8 seropositive AIDS patients (21, 229). From these observations, RRV is considered to be the rhesus macaque homologue of HHV-8.

Studying the functions of viral ORFs can lend insight into their roles during viral infection and disease progression. ORFs likely contributing to RRV pathogenesis have begun to be studied and include those that encode for a viral IL-6 homologue (vIL-6) and a viral G protein-coupled receptor (vGPCR). It has been demonstrated that RRV vIL-6 and vGPCR behave similarly to their counterparts in HHV-8, supporting B cell proliferation (109) and promoting cellular transformation (71), respectively. R1 of RRV has also been analyzed, and was determined to possess

transforming potential, and to promote lymphocyte activation (57, 58). Another RRV ORF that likely promotes viral pathogenesis is R15, which encodes a homologue of human CD200.

Human CD200 is expressed as a membrane glycoprotein that is found on the surface of many cell types including epithelium, neurons, and lymphocytes (14, 29, 223). Structurally, CD200 contains two immunoglobulin domains, a transmembrane domain, and a very short cytoplasmic domain lacking any identifiable signaling motifs. To elicit an effect, CD200 binds to its receptor, CD200R, which is largely restricted to the surface of cells of myeloid lineage (231). Ligation of CD200R results in a decrease in the production of type 1 (inflammatory) cytokines such as tumor necrosis factor (TNF), and a shift toward a type 2 (anti-inflammatory) cytokine response from the cells displaying CD200R (102, 170).

HHV-8 K14 also encodes a vCD200 homologue whose function resembles that of human CD200. Specifically, HHV-8 vCD200 downmodulates macrophage activation through binding to CD200R on activated macrophages, thereby reducing the level of TNF production. Foster–Cuevas *et al.* also demonstrated that HHV-8 vCD200 is expressed on the surface of latently infected B lymphocytes following lytic cycle induction (77). Recently, myxoma virus M141R encoded vCD200 has been investigated and the importance of myxoma virus vCD200 in pathogenesis was highlighted. In this study, European rabbits overcame infection with a modified myxoma virus lacking vCD200, while their counterparts, infected with wild-type myxoma did not recover (33).

In this report we investigate the expression and function of RRV vCD200 encoded by ORF R15. Here we demonstrate that RRV vCD200 is a glycoprotein sharing 30% amino acid identity with human CD200. Despite the low sequence identity, RRV vCD200 is predicted to share similar structural arrangement to human CD200, containing two immunoglobulin domains, a transmembrane domain and a short cytoplasmic domain, which is consistent with a protein expressed on the cell surface, as detected with a monoclonal antibody directed against vCD200. Additionally, a recombinant RRV vCD200 was capable of affecting cytokine production from activated human monocyte-derived macrophages and primary rhesus macaque macrophages.

Our previous work suggests that RRV vCD200 is expressed not only as a membrane-bound protein, but also as a truncated version, which is capable of being secreted during infection (169). Therefore, the potential exists for a large-scale regulation of the cytokine environment surrounding infected cells, reducing the levels of type 1 cytokine production from myeloid cells, thereby promoting the persistence of RRV infected cells.

MATERIALS AND METHODS

CD200 alignments. Clustal W protein alignments were performed using sequences from GenBank for human CD200 (Accession # NM 005944), RRV vCD200 (Viral Genome Accession #AF083501), and HHV-8 vCD200 (Viral Genome Accession # NC 003409). Immunoglobulin V-Type domains were predicted through the use of CD-Search (139). Transmembrane regions were predicted through the use of TM Pred software (103), and the SignalP program was utilized to predict signal sequences within human CD200, RRV and HHV-8 vCD200 (158).

Cells and virus. Human THP-1 cells were maintained in Roswell Park Memorial Institute (RPMI) 1640 media (Mediatech, Herndon, VA) supplemented with 10% fetal bovine serum (FBS) (HyClone, Logan, UT). Primary rhesus fibroblasts (Swanson 1998) were grown in Dulbecco's modification of Eagle's media (DMEM) (Mediatech) supplemented with 10% FBS (HyClone). Chinese hamster ovary (CHO) cells were grown in F12K media (Mediatech) containing 5% FBS (HyClone). Differentiation of THP-1 cells was achieved through overnight incubation of cells with 160 nM phorbol 12-myristate 13-acetate (PMA) (Sigma, St. Louis, MO). All cells were cultivated in a CO₂ incubator (37°C, 5%CO₂). RRV stocks were obtained by infection of primary rhesus fibroblasts with RRV₁₇₅₇₇ clone #3.

Fc fusion protein generation. R15 sequence corresponding to the predicted extracellular domain of RRV vCD200 was amplified using PCR from RRV₁₇₅₇₇ cosmid 28-2 with primers specific for this region (Forward EcoRI primer: 5'-

GAATTCTCAATTATGTCGGGAGGAA-3', Reverse BstEII primer: 5'-
GGTGACCGCGTAGTGGCTCGTCC-3'). The DNA sequence corresponding to the
extracellular domain of human CD200 was amplified using PCR from a plasmid
containing CD200 (a generous gift from A. N. Barclay, University of Oxford, Oxford,
UK) with primers specific for this region (Forward EcoRI primer: 5'-
GAATTCTCAATTATGGGCAGTCCGGTGATCAGG-3', Reverse BstEII primer: 5'-
GGTCACCCCTTTGTTGACGGTTTGCTTA-3'). Within primer sequences,
restriction sites are underlined and Kozak sequences are in italics. PCR products were
initially cloned into pCRII-Topo (Invitrogen Life Technologies, Carlsbad, CA) for
sequence analysis. Further subcloning allowed for the generation of Fc fusion
constructs (Fc construct kindly provided by A. Weinberg, Earle Chiles Research
Institute, Portland, OR) and Fc fusion constructs were finally subcloned into
pcDNA3.1(-) (Invitrogen Life Technologies) between EcoRI and KpnI restriction
sites for expression in CHO cells.

Fc fusion protein production and purification. Subconfluent CHO cells were
transiently transfected in 60 mm dishes (Corning Incorporated Life Sciences, Acton,
MA) using Transit LT1 reagent (Mirus, Madison, WI) with 3 µg of DNA per dish.
Transfections were carried out under serum-free conditions to facilitate subsequent
purification of Fc proteins from cell supernatants. CHO supernatants were collected
each day for four days following transfection, and cell debris was removed from
supernatants by centrifugation. Batches of supernatants were purified through binding
of Fc fusion proteins to a column packed with protein G Sepharose 4 Fast Flow

(Amersham Biosciences, Piscataway, NJ). Fc fusion proteins were eluted from the column with low pH (pH=2.8). Purified fractions were pooled, dialyzed against PBS, and concentrated using Amicon ultra centrifugal filter devices (Millipore, Bedford, MA). Concentrations of Fc fusion proteins were determined with a Bradford Assay (Bio-Rad Laboratories, Hercules, CA).

RRV vCD200-Fc characterization. Native and denatured samples of purified RRV vCD200-Fc were run on a 10% polyacrylamide gel and subjected to standard Western blot procedure. Briefly, the 10% polyacrylamide gel was transferred to a nitrocellulose membrane, and probed with an Fc-specific antibody conjugated to horseradish peroxidase (HRP) (Sigma). RRV vCD200-Fc was treated with PNGase F (New England Biolabs, Beverly, MA) following manufacturer's specifications, allowing the reactions to proceed for 10 and 60 minutes. PNGase F treated samples were analyzed by standard Western blot procedure, as above, with an anti-Fc antibody conjugated to HRP (Sigma).

Derivation of 11B8.2.2.6 hybridoma (anti-RRV vCD200). Balb/c female mice (8 week old females) were immunized intraperitoneally three times with 25-50 µg recombinant vCD200-Fc. The mouse spleen cells were then fused with NS-1 myeloma cells using 50% polyethylene glycol to establish hybridomas (60). Cell lines positive in ELISA screening for vCD200 were subcloned 2-3 times to ensure monoclonality. Scale-up production of antibody by cloned cells was accomplished in an Integra Biosciences CELLline system CL1000 bioreactor, according to the

instructions of the manufacturer. The 11B8.2.2.6 antibody was purified using a combination of thiophilic (18) and cation exchange chromatography.

Biotinylation of Antibodies. Monoclonal antibodies, specific for RRV vCD200 (clone 11B8.2.2.6), and mouse IgG₁ (clone 11711, R & D systems, Minneapolis, MN) were biotinylated following the manufacturer's guidelines of the labeling kit from Pierce Biotechnology (Rockford, IL).

Immunofluorescence Assay on RRV infected cells. Primary rhesus fibroblasts were plated onto Lab-Tek II chamber slides (Nalge Nunc International, Naperville, IL) the day before infection. Fibroblasts were infected with RRV₁₇₅₇₇ at a multiplicity of infection (MOI) of 2.0. 52 hours post RRV infection, primary rhesus fibroblasts were fixed with 4% paraformaldehyde at room temperature for 10 minutes. Following fixation, cells were washed, dehydrated, dried at room temperature, and baked onto slides at 58°C overnight. Slides were then stored at -80°C. From the freezer, cells were first hydrated then extensively blocked utilizing biotin and avidin blocking reagents (Vector Labs, Burlingame, CA) for 15 minutes at room temperature, followed by incubation with 10% BSA at 37°C for 10 minutes, and final blocking with mouse IgG₁ (200 µg/mL, clone 11711, R & D systems) for one hour at room temperature. RRV infected primary rhesus fibroblasts were stained with 50 µg/mL of biotinylated anti-RRV vCD200 antibody (clone 11B8.2.2.6) or with 50 µg/mL of biotinylated mouse IgG₁ as an isotype control. Uninfected primary rhesus fibroblasts were also stained with 50 µg/mL of biotinylated anti-RRV vCD200 antibody. Cells

were incubated overnight at room temperature with primary antibodies in a humidified chamber. Following washing, a biotin amplification step was employed using a Vectastain Elite ABC Kit (Vector Laboratories). Cells were then incubated with streptavidin-conjugated Quantum Dot 655 (Quantum Dot, Hayward, CA) for 30 minutes at room temperature. Slides were then washed, dehydrated, mounted, and visualized with a Nikon Eclipse E800 microscope (Melville, NY) used in conjunction with the Bio-Rad Radiance 2100/Lasersharp 2000 confocal microscopy system to capture raw images. A helium/neon laser with a laser line of 543 nm was used to excite Quantum dot 655, and the emitted light was captured in the 650-660 nm range. Raw data generated with the Lasersharp 2000 software was post processed with ImageJ image analysis software (ver1.32j, W. Rasband, National Institutes of Health). Images were captured using a 40X objective lens (Nikon).

Examining levels of CD200R RNA within THP-1 cells. Reverse transcription PCR (RT-PCR) was performed to amplify CD200R from RNA collected from THP-1 cells that were untreated or treated with PMA. Briefly, 500 ng of RNA was used as template for each RT-PCR using the Superscript III One-Step RT-PCR system (Invitrogen Life Technologies), following manufacturer's instructions. Reactions containing Vent DNA polymerase in the place of RT served as controls to demonstrate the absence of DNA contamination of RNA in amplifying glyceraldehyde-3-phosphate dehydrogenase (GAPDH). Primers used to amplify CD200R: Forward: 5'-ATGCTCTGCCCTTGGAGAAC-3', Reverse: 5'-TCTATTCCTGTTTTGAAACA-3'. GAPDH primers: Forward: 5'-TTCATTGACCTCAACTACATG-3', Reverse: 5'-GTGGCAGTGATGGCATGGAC-

3'. Reaction products were run on a 1.7% agarose gel and visualized with ethidium bromide staining. Quantitation of fold increase in CD200R message was calculated with Kodak 1D Image Analysis Software (Kodak Image Station 440 CF, New Haven, CT).

Examination of CD200R expression on the surface of THP-1 cells. THP-1 cells were plated into Lab-Tek II chamber slides (Nalge Nunc International) at 1.0×10^5 cells per chamber and were incubated overnight with PMA. Cells were then fixed with 4% paraformaldehyde for 10 minutes at room temperature, and blocked with biotin and avidin blocking reagents (Vector Labs) for 15 minutes at room temperature, and 10% BSA at 37°C for 10 minutes. Next, THP-1 cells were stained with either a biotinylated CD200R antibody (OX-108, Serotec, Raleigh, NC) or with a biotinylated mouse IgG₁ (clone 11711, R&D Systems) at 1.0 µg/mL overnight at room temperature. Finally, THP-1 cells were incubated with streptavidin-conjugated Quantum Dot 655 (Quantum Dot) for 30 minutes at room temperature, and visualized with a Zeiss Axioskop2 plus microscope (Thornwood, NY) equipped with a 655 nm filter, utilizing a 20X objective.

Assessing function of RRV vCD200-Fc. THP-1 cells were plated into wells of 24 well dishes (Corning Incorporated Life Sciences) at 1.88×10^5 cells in 0.25 mL per well in the presence of PMA to induce maturation. Following PMA treatment, adherent cells were washed and incubated with a blocking anti-Fcγ receptor I antibody (αhuCD64, clone 10.1, R & D Systems) for 30 minutes at 37°C/5% CO₂.

Cells were washed, then incubated with a mixture of IFN- γ (100 U/mL, R & D Systems) and Fc proteins (90 pM), either Fc fragment of human IgG (Chemicon, Temecula, CA), human CD200-Fc, or RRV vCD200-Fc. Each Fc treatment was carried out in duplicate tissue culture wells. At 2 and 4 hours following the addition of Fc proteins, THP-1 cells were collected in TRI Reagent (Sigma) for subsequent RNA isolation. Supernatants of THP-1 cultures were collected at 22 hours post-addition of Fc proteins. Cellular debris was removed from supernatants through centrifugation.

TNF ELISA. Cell-free supernatants were assayed for levels of TNF using an ELISA according to manufacturer's specifications (BD Pharmingen, San Diego, CA). Mean fold change in levels of TNF (range for THP-1= 3000-7000 pg/mL, range for rhesus macrophages = 2-20 pg/mL) are represented as bars +/- standard deviations (SD). Mean fold change of cells treated with Fc alone was used as a reference, with the fold change = 1. Results shown are representative of three experiments.

qRT-PCR. Total RNA was obtained from THP-1 cultures following incubation with Fc proteins using TRI Reagent (Sigma) according to manufacturer's specifications. 2 μ g of purified RNA was treated with DNase I (Invitrogen Life Technologies) per manufacturer's instructions, and used in reverse transcriptase reactions with Superscript II reverse transcriptase (Invitrogen Life Technologies) to generate cDNAs. To detect changes in TNF expression, 50 ng of cDNA from treated THP-1 cells, was used in quantitative PCR (ABI 7700 sequence detection system, Applied

Biosystems, Foster, CA) with primers specific for TNF (Forward: 5'-GCCCCCAGAGGGAAGAGTTC-3', Reverse: 5'-GCTTGAGGGTTTGCTACAACATG-3') or GAPDH (Forward: 5'-TGACCTCAACTACATGGTTTAC-3', Reverse: 5'-AGGGATCTCGCTCCTGGAA-3') (generous gifts from M. Jordanov, OHSU). SYBR green (Applied Biosystems) intercalation into double stranded DNA PCR products is measured throughout the reaction and during the exponential phase of each reaction, an arbitrary cycle threshold (c_t) is determined for each reaction. c_t values from GAPDH reactions are used for normalization of TNF levels, allowing for comparison of amounts of TNF transcripts between cells treated with varying Fc proteins. Differences in the levels of transcripts encoding TNF are plotted as mean fold change, comparing all experimental values to those from cells treated with Fc alone (fold change = 1). Results shown are representative of three experiments.

Statistical Analyses. Statistical comparisons were made between the three Fc treatments (Fc, HuCD200-Fc, RRV vCD200-Fc) using a repeated measures ANOVA analysis. Individual comparisons of vCD200-Fc or HuCD200-Fc treatments with Fc control treatments were performed with Tukey-Kramer post-test (GraphPad InStat software v.3.0a).

Isolation and Culturing of Rhesus Macaque Macrophages. Peripheral blood mononuclear cells (PBMCs) were isolated from 10 mL of blood that was collected from expanded specific pathogen free (SPF) rhesus macaques, naïve for RRV,

through density gradient centrifugation on Histopaque-1077 (Sigma). PBMCs from individual animals were then washed and plated into four 35 mm Primaria dishes (Becton Dickinson Labware, Franklin Lakes, NJ) with Iscove's DMEM (Mediatech) containing 10% FBS and concavalin A (conA) (5 μ g/mL, Sigma). 18 hours following conA stimulation, lymphocytes were washed from dishes and the remaining adherent macrophages were cultured in 60% AimV (Invitrogen Life Technologies), 30% Iscove's DMEM (Mediatech), and 10% FBS. Every third day, a 50% media change was performed (198). Seven days following conA stimulation of PBMCs, macrophages were incubated with Fc proteins (Fc alone, human CD200-Fc, or RRV vCD200-Fc) similar to the method for THP-1 cells except that Fc proteins were added at 180 pM to account for higher cell density, and cell supernatants were collected at 4h.

RESULTS

CD200 alignments. Comparing amino acid sequences between human CD200 and RRV vCD200, it was determined that these proteins are 30% identical, while the HHV-8 vCD200 shares 28% identity with RRV vCD200 and 26% identity with human CD200 (Figure 3.1). Despite low sequence identity, the structural organization of these three proteins is very similar, indicating that the structural components of these proteins are conserved through evolution and must play important roles for function. Specifically, human CD200 and RRV vCD200 have overlapping transmembrane domains, and very similar locations of their V-type immunoglobulin-like domains. Importantly, RRV vCD200 sequence contains the two cysteine residues that have been reported to be involved in disulfide bond formation within the V-type immunoglobulin-like domain (33).

Purified RRVvCD200-Fc. To facilitate purification of RRV vCD200, we generated a fusion protein consisting of the predicted extracellular domain of vCD200 (amino acid 1 - 228) fused in frame with the Fc fragment of human IgG₁. This fusion (termed RRV vCD200-Fc) was expressed from transiently transfected CHO cells under serum free conditions, and each day for four days following transfections, cell supernatants were collected. RRV vCD200-Fc was purified from cleared supernatants with protein G conjugated agarose beads. A low pH buffer was employed to elute the Fc fusion proteins from the beads.

Purified vCD200-Fc was subjected to Western blot analysis with an Fc-specific antibody to confirm both the size of the fusion protein and that the Fc

fragment of IgG₁ within the fusion protein allows for dimerization of vCD200, which has been demonstrated to be critical for maintaining the function of soluble CD200 molecules (77). Dimerization of RRV vCD200-Fc is achieved following expression from CHO cells, and this is demonstrated when comparing purified protein samples run under native and denaturing conditions, with the monomeric form of vCD200 only present in the denatured sample (Figure 3.2, lanes 1 and 2). RRV vCD200-Fc has a predicted molecular weight of ~53 kDa and contains several predicted N-linked glycosylation sites, which likely contributes to the higher molecular weight (Figure 3.2, lane 2). The core protein size can be visualized through treatment of vCD200-Fc with PNGaseF to remove N-linked sugars (Figure 3.2, lanes 3 and 4). No O-linked glycosylation sites are predicted, and treatment of vCD200-Fc with O-Glycosidase had no effect on protein migration (data not shown). The same purification scheme was employed for the purification of HuCD200-Fc and this protein also exists as a dimer in our hands (data not shown).

Expression of RRV vCD200 during RRV lytic infection. Mice were immunized with purified RRV vCD200-Fc to generate a hybridoma clone that secreted monoclonal antibodies specific for vCD200. These monoclonal antibodies allow for the detection of vCD200 during RRV infection. We have previously demonstrated that R15, the ORF that encodes for vCD200, is transcribed as a late gene (169). Since RRV induces a lytic infection in primary rhesus fibroblasts, infected cells were fixed at 52 hours post infection to maintain the integrity of the infected cells. To examine surface staining of RRV infected fibroblasts (MOI=2.0), cells were fixed with

paraformaldehyde, and stained with either a monoclonal antibody generated against vCD200 or with an isotype control antibody. Confocal imaging of stained cells revealed vCD200 expression on the surface of RRV infected fibroblasts, indicating that this protein is synthesized during lytic RRV infection, and that it is at least partially localized to the surface of infected cells (Figure 3.3A). Specific staining was absent from RRV infected cells stained with the isotype control antibody (Figure 3.3B), as well as from uninfected cells stained with the anti-vCD200 antibody (data not shown).

Assessing function of RRV vCD200-Fc. As vCD200 is expressed on the surface of infected fibroblasts during lytic infection, we sought to determine if RRV encodes a functional CD200 homologue. To accomplish this, the human monocytic cell line, THP-1, was first analyzed for expression of CD200 receptor (CD200R). Following stimulation with PMA, levels of CD200R RNA are upregulated 2.6 fold by semi-quantitative RT-PCR, compared to non-stimulated THP-1 cells when normalized to control GAPDH RNA levels (Figure 3.4A). Further confirmation of CD200R expression was evidenced by immunofluorescence staining (Figure 3.4B), which verified surface expression and the suitability of THP-1 cells for *in vitro* studies.

To examine function of RRV vCD200-Fc, THP-1 monocyte-derived macrophages were incubated with a mixture of IFN- γ (for activation) and Fc proteins for varying amounts of time. Specifically, cells were treated with Fc alone, human CD200-Fc, or RRV vCD200-Fc. At early time points (2 hours and 4 hours), cells were collected and harvested for RNA to detect expression changes in levels of the

type 1 cytokine TNF transcript. Should RRV vCD200-Fc behave as a true homologue of CD200, the levels of TNF message should be decreased compared to cells treated with Fc alone. Utilizing quantitative real-time reverse transcription PCR (qRT-PCR) with cDNAs generated from THP-1 RNA, we observe a 0.29 fold decrease, and a 0.68 fold decrease in TNF transcripts from THP-1 that have been incubated with RRV vCD200-Fc for 2 hours and 4 hours, respectively compared to cells treated with Fc alone (Figure 3.5A). Initially, downregulation of TNF messages was highest in cells treated with human CD200-Fc (fold decrease = 0.51), however, by 4 hours the levels of downregulation as a result of RRV vCD200-Fc treatment were similar to those resulting from incubation of THP-1 with human CD200-Fc (fold decrease = 0.64) (Figure 3.5A). As we observed significant differences in levels of TNF message at 2 and 4 hours post-addition of human CD200-Fc and RRV vCD200-Fc, we next examined the effect on TNF protein production from these cells. An ELISA was used to measure levels of TNF in the supernatants of treated THP-1 cells. At 2 hour and 4 hour time points, no significant differences were detected between cells that had been treated with Fc and those treated with human CD200-Fc or RRV vCD200-Fc (data not shown). However, at 22 hours following addition of Fc proteins, we did observe differences in levels of TNF in supernatants. THP-1 cells incubated with RRV vCD200-Fc displayed a 0.36 fold decrease in TNF levels, and cells incubated with human CD200-Fc displayed a 0.47 fold decrease in secreted TNF levels compared to Fc controls (Figure 3.5B).

To examine the effect of RRV vCD200-Fc on a more native cell type than human THP-1 cells, primary rhesus macrophages were isolated from PBMCs from

four specific pathogen free (SPF) animals that were naïve for RRV infection. Here, TNF levels in cell supernatants were measured 4 hours following incubation with Fc proteins. Similar to what was observed in human cells, primary rhesus macrophages incubated with RRV vCD200-Fc displayed reduced levels of TNF in the supernatant (fold decrease = 0.88) versus cells treated with Fc alone. Human CD200-Fc had a lesser effect compared with vCD200-Fc, but nonetheless reduced levels of secreted TNF (fold decrease = 0.71) (Figure 3.6), suggesting that RRV vCD200 is functionally more potent than human CD200 on primary rhesus macrophages.

DISCUSSION

For viruses to successfully infect their host, replicate, and ultimately generate progeny, they must evade the host immune response. Human CD200 has been demonstrated to have immunomodulatory function, controlling the activation of myeloid cells (102, 155, 170, 231). Therefore, a virus incorporating a gene encoding a CD200 homologue into its genome would have a clear advantage over a virus lacking this molecule in evading the host immune surveillance. In fact, evolution has supported the propagation of viruses encoding vCD200 molecules within various families, including *Herpesviridae* (RRV, HHV-6, HHV-7, HHV-8, the English strain of rat CMV), *Poxviridae* (Myxoma virus, Yaba-like disease virus, Sheep pox virus, Shope fibroma virus, Lumpy skin disease virus, Yaba-monkey tumor virus), and *Adenoviridae* (Duck adenovirus) (33, 77). To date, only vCD200 homologues from HHV-8 and myxoma virus have been characterized. HHV-8 K14 encoded vCD200 has been reported to bind CD200R on human macrophages, reducing levels of TNF secretion (77). The role of myxoma virus vCD200 in pathogenesis has recently been investigated, where it was found that rabbits that would normally succumb to myxoma infection were able to survive infection with a virus lacking vCD200 (33). This lends strong evidence to the importance of CD200-like molecules in controlling the host immune response during infection to allow for increased viral propagation.

In this report we evaluate the expression and function of RRV encoded vCD200. For these studies, we utilized a fusion protein in which the predicted extracellular domain of RRV vCD200 was fused with the Fc portion of human IgG₁. We have produced a vCD200-specific monoclonal antibody that detected expression

of vCD200 on the surface of RRV infected primary rhesus fibroblasts indicating that this protein is expressed during lytic infection. This expression agrees with our previous reported expression of epitope-tagged RRV vCD200 from cDNA constructs that localized to the surface of transfected cells (169). In addition, we previously reported on a transcriptional splicing event that results in the production of a soluble form of vCD200 (169). Therefore, we assume that two forms of vCD200 could exist during infection: a membrane-bound form and a secreted form. While we were able to detect membrane-bound form of vCD200 during RRV infection, our antibody did not recognize the secreted version of vCD200 in Western blot analysis despite recognition of the secreted form from transfected cells (data not shown). We postulate that the secreted form of vCD200 may be expressed at low levels during lytic infection, or may be modified in some way during infection, to mask the epitope that is recognized by our monoclonal antibody. HHV-8 encoded vCD200 has also been demonstrated to localize to the surface of latently-infected B lymphocytes following induction to undergo viral lytic replication (77).

Although human monocyte-derived macrophages are believed to express CD200R (230), our studies used a transformed monocytic cell line that has not been evaluated for CD200R expression. It has been suggested that the human monocytic cell line, U-937, lacks expression of this receptor (77), therefore we felt this to be an important determinant in choosing a cell line for our studies. Following confirmation of CD200R on PMA treated THP-1 cells, we subsequently assessed the function of RRV vCD200-Fc.

While amino acid sequence identity is not strikingly high between RRV vCD200 and HuCD200, the function of RRV vCD200 appears to resemble that of HuCD200. Specifically, both HuCD200-Fc and RRV vCD200-Fc were found to reduce expression of the type 1 cytokine tumor necrosis factor (TNF) from human monocyte-derived macrophages at the transcriptional level. Incubating cells with HuCD200-Fc was a control for reduction in TNF levels, and at two hours following incubation of cells with Fc proteins, HuCD200-Fc was more effective than RRV vCD200-Fc in reducing TNF transcripts, but by four hours following addition of Fc proteins, changes in TNF transcripts were comparable between HuCD200-Fc and RRV vCD200-Fc treatments. One possible explanation for the apparent lag in effectiveness of RRV vCD200 is that vCD200 has a lower affinity for human CD200R than HuCD200, as vCD200 is thought to have evolved to bind CD200R of rhesus macaque origin. Unfortunately, the rhesus macaque CD200R has not been identified, therefore, ideas of differing binding affinities are merely speculative. Levels of TNF secreted from human monocyte-derived macrophages were reduced to similar degrees from cells incubated with HuCD200-Fc and RRV vCD200-Fc compared with controls. From these studies we can conclude that RRV vCD200-Fc behaves similarly to HuCD200-Fc in reducing expression of the type 1 cytokine TNF from CD200R⁺ human macrophages. However, RRV vCD200-Fc appeared to have a stronger effect than HuCD200-Fc in reducing TNF expression from primary rhesus macrophages, which may correlate with differing affinities of HuCD200-Fc and RRV vCD200-Fc for the rhesus macaque CD200R.

Unfortunately, we were unsuccessful in blocking the biological action of RRV vCD200-Fc through the use of antibodies directed against CD200R or those directed at vCD200. More specifically, the commercially available CD200R antibody (OX-108), and our monoclonal antibody, which specifically recognizes vCD200 in immunofluorescence, were unable to relieve the inhibition in TNF expression from HuCD200-Fc or vCD200-Fc treated THP-1 cells (data not shown). We can, therefore speculate that our monoclonal antibody recognizes an epitope outside of the identified regions involved in the interaction with CD200R (99).

Collectively, we understand that during lytic infection, RRV R15 encodes a functional vCD200 homologue that has capabilities to modulate activation of myeloid cells. Specifically, during infection, RRV vCD200 could inhibit activation of infiltrating monocytes and macrophages, reducing their production of inflammatory cytokines that are deleterious to RRV infected cells. Unlike what has been demonstrated for HHV-8 vCD200, RRV encodes two forms of vCD200: a soluble secreted form produced by transcriptional splicing, and an unspliced membrane-bound form. Expressing two forms of this immunomodulatory protein allows for greater protection of an infected cell from surrounding and infiltrating myeloid cells. An infected cell expressing RRV vCD200 on its surface may be able to control activation of myeloid cells that directly interact with infected cells, while the secreted vCD200 could restrict activation of neighboring and infiltrating myeloid cells that could otherwise respond to RRV infection. Since expression of RRV vCD200 occurs late during lytic infection (169), the presence of a secreted vCD200 is advantageous to RRV as the infected cell will soon be destroyed. Further, by producing a secreted

immunomodulatory protein that can control the activation of myeloid cells, neighboring infected cells may be protected from host immune cell destruction, allowing these cells to complete of the viral lytic cycle and produce viral progeny. In the case of HHV-8, however, K14 expression has been reported to occur early during lytic infection (47, 116, 153), therefore, this molecule might have more time to elicit its local effect on myeloid cells directly encountering an infected cell before the infected cell is lysed.

As RRV vCD200 shares immunomodulatory function with HHV-8 vCD200, the role of this viral ORF in viral-mediated pathogenesis can be elucidated in a closely related animal model, the RRV/SIV-infected rhesus macaque. For example, utilizing the rhesus macaque model of RRV/SIV co-infection along with BAC technology to generate an R15 knockout virus, the function of RRV vCD200 may be evaluated *in vivo*. In addition, the possibility exists that the secreted form of vCD200 could be tested in transplant models as a potential therapeutic agent to enhance graft survival, a finding that has been demonstrated for cellular CD200 in rodent transplant models (87, 92, 93, 236).

ACKNOWLEDGEMENTS

This work was supported by NIH grants CA75922 and RR00163. We acknowledge D. Cawley for the production of monoclonal antibodies against vCD200. We are grateful for technical assistance with qRT-PCR experiments and data analysis from the laboratory of M. Jordanov. Also, we thank K. Langlais for technical assistance with confocal microscopy and statistical analyses, and R. Estep for thoughtful discussions.

Figure 3.1. ClustalW protein alignments of human CD200 (huCD200) and viral CD200 homologues (vCD200), RRV vCD200 and HHV-8 vCD200. There is 30% sequence identity between RRV vCD200 and huCD200, 26% identity between HHV-8 vCD200 and huCD200, and 28% identity between vCD200s. huCD200 V-like Ig domain is noted with a fine solid line above the sequence, and the transmembrane domain of huCD200 is noted with a dashed line above the sequence. Cysteine residues important for disulfide bond formation within Ig domains are noted with (*). Signal peptide cleavage sites are noted with (v) along with R for RRV vCD200, H for huCD200, and K for HHV-8 vCD200.

RRV WCD200
 HUCD200
 HHV-8 WCD200

5 10 15 20 25 30 35 40 45 50

M E R L V I R M P F C H S G G I T L L L L L A T L A T V R C A L Q T H Y A A V P - - - V H S T A S I G
 M S S L F I S L P W M A A V V L C T A Q V V V I Q P A Y R K D K I N I T Q L G
 M S S L F I S L P W M A A V V L C T A Q V V V I Q P A Y R K D K I N I T Q L G

RRV WCD200
 HUCD200
 HHV-8 WCD200

55 60 65 70 75 80 85 90 95 100

C V L T T P H D V L I V T V Q E K Q E S P P P V H V A T Y S S E A G T V V Q P P F A G R V D I P E H K
 C S L Q N A Q E A L I V T V Q E K Q E S P P P V H V A T Y S S E A G T V V Q P P F A G R V D I P E H K
 C A I T P R A D I V S V T V Q E K Q E S P P P V H V A T Y S S E A G T V V Q P P F A G R V D I P E H K

RRV WCD200
 HUCD200
 HHV-8 WCD200

105 110 115 120 * 125 130 135 140 145 150

L T R T T L K F F N A T L E D E G C T I C I F H A F G V G E L S G T A C L I T V Y V P L S M S V T F Y
 L Q N S T I T F W N I T L E D E G C T M C L F H T F G F G E K I S G T A C L I T V Y V P L S M S V T F Y
 L W N S T I V I H N L A V D D E G C Y L C I Y N S F G G R Q V S C T A C L E V T S P P T I G H V V V N

RRV WCD200
 HUCD200
 HHV-8 WCD200

155 160 165 170 175 180 185 190 195 200

P P I N P T Q L V C R A E A S P A P S V N W T G V P P E L C S E P E V P R P N G T I L V V G R C N
 F S E D H L I N I T C S A T A R P A P M V F W K V P R S G I E N S T V T L S H P H G T I S V T S I L H
 S T E D A D T V T C L A T I G R P P P N V T W A A P W N N A S S T Q E Q E T D S D G L T V A W R T V R

RRV WCD200
 HUCD200
 HHV-8 WCD200

205 210 215 220 225 230 235 240 245 250

V T S V V D P E D L E N A T C I V T H I G - - - G L A A A R P L D - - - P V F S D P L E G T S H Y
 I K D P K N Q V G K E V I C Q V L H L G - - - T V T D D F K Q T V N K G Y W F S V P L L I S I V S
 L P R G D N T T P S E G I C L I T W G N E S I S I P A S I Q G P L A H D L P A A Q G T L A G V A I T

RRV WCD200
 HUCD200
 HHV-8 WCD200

255 260 265 270 275 280 285 290 295 300

V V G V V A A A V L G I F L T G V - - - F L Y R S M
 L V I L L V L I S I L L Y W K R H R - - - N Q P D R E F
 L V G L F G I F A L H H C R R K Q G G A S P T S D D M D P L S T Q

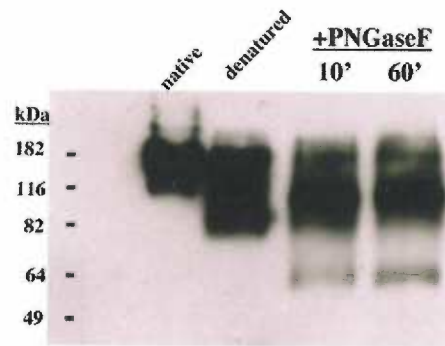


Figure 3.2. Fc Western blot of purified RRV vCD200-Fc. Purified vCD200-Fc samples were run under native and denaturing conditions to determine if vCD200-Fc dimerizes. Under native conditions, vCD200-Fc migrates slower than the denatured sample, suggesting that this Fc fusion protein dimerizes (lanes 1 and 2). PNGaseF treatment of native protein reveals that vCD200-Fc is N-linked glycosylated, as the core protein size (~53 kDa) is revealed following treatment (lanes 3 and 4).

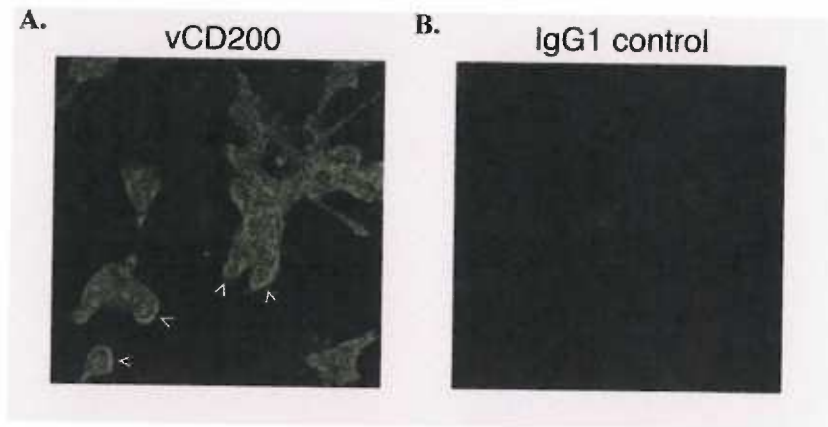


Figure 3.3. Immunofluorescence of RRV infected fibroblasts. (A) Specific staining of vCD200 is observed on the surface (<) of infected cells 52 hours post infection. (B) No specific staining was observed when incubating infected cells with the isotype control antibody. Images are 281 microns x 281 microns.

Figure 3.4. CD200R expression within THP-1 cells. (A) RT-PCR demonstrating that following maturation of THP-1 cells through overnight PMA treatment, there is a 2.6 fold increase in CD200R message relative to GAPDH products. (B)

Immunofluorescence of PMA treated THP-1 cells to demonstrate surface expression of CD200R with a biotinylated CD200R specific antibody. No specific staining was observed for the biotinylated isotype control antibody. Images are 510 microns x 385 microns.

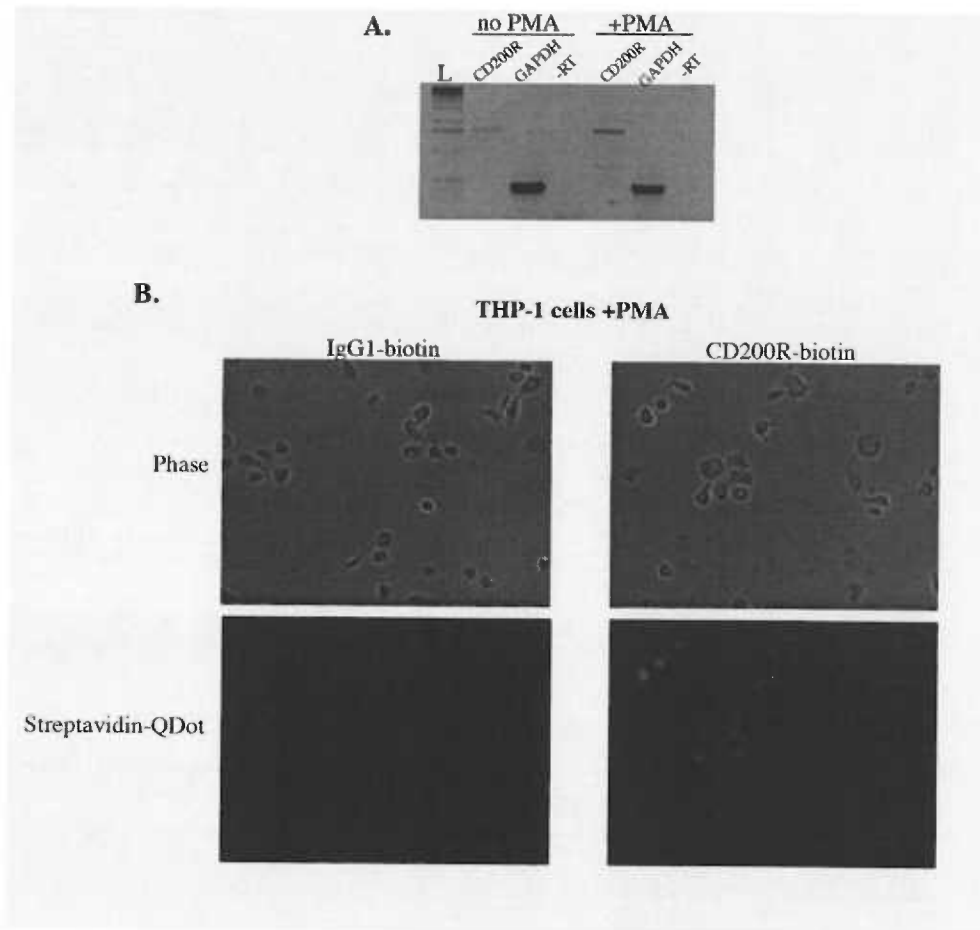
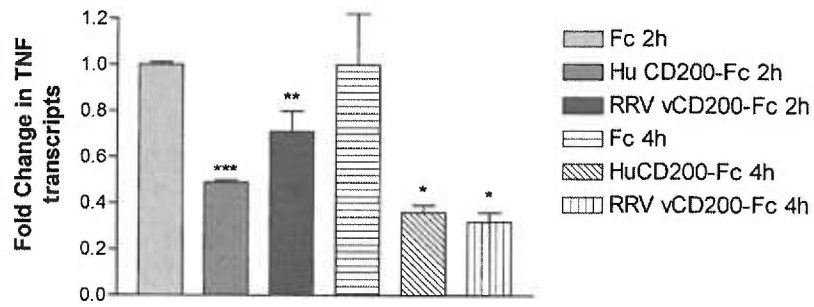
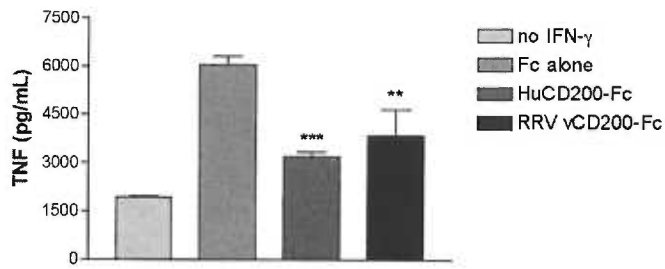


Figure 3.5. RRV vCD200-Fc downregulates TNF expression in IFN- γ treated THP-1 cells. (A) qRT-PCR to examine levels of TNF transcripts 2 and 4 hours following incubation of IFN- γ treated THP-1 cells with Fc proteins (Fc alone, HuCD200-Fc, or RRV vCD200-Fc). At 2h following incubation with Fc proteins, IFN- γ treated THP-1 cells incubated with HuCD200-Fc display 0.51 fold decrease in levels of TNF transcripts in comparison to cells treated with Fc alone. IFN- γ treated THP-1 cells incubated with RRV vCD200-Fc had a 0.29 fold decrease in TNF transcripts compared to cells incubated with Fc alone. By 4 hours, the reduction in TNF transcripts was comparable between HuCD200-Fc and RRV vCD200-Fc, with 0.64 fold and 0.68 fold decrease, respectively. (B) ELISA to measure levels of secreted TNF in IFN- γ treated THP-1 cell supernatants 22 hours following incubation with Fc proteins. In comparison to cells treated with Fc alone, HuCD200-Fc treatment of IFN- γ treated THP-1 cells resulted in a 0.47 fold decrease in secreted cytokine levels. RRV vCD200-Fc treatment of IFN- γ treated THP-1 cells resulted in a 0.36 fold decrease in secreted TNF compared to cells incubated with Fc alone. Results shown are representative of three experiments. * denotes a significant difference compared with Fc treatment ($p < 0.05$), ** denotes a very significant difference compared with Fc treatment ($p < 0.01$), *** denotes an extremely significant difference compared with Fc treatment ($p < 0.001$).

A.



B.



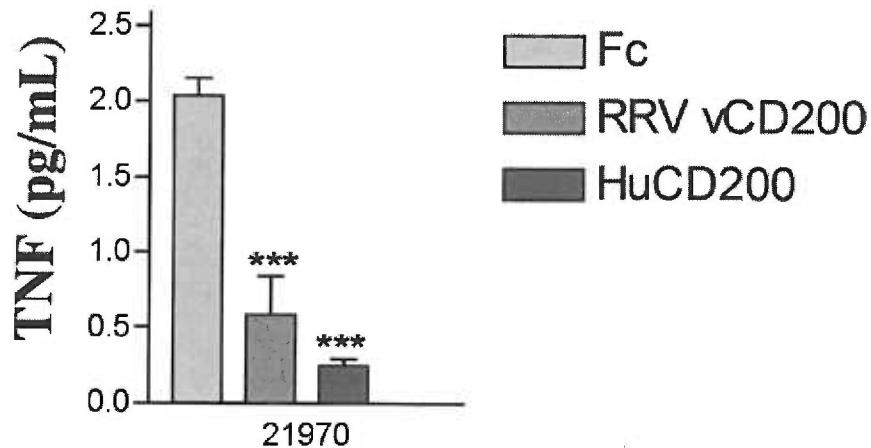


Figure 3.6. TNF ELISA from IFN- γ treated primary rhesus macrophage supernatants. Following four-hour incubations with Fc proteins, supernatants of IFN- γ treated rhesus macrophages were assayed for TNF levels. RRV vCD200-Fc treatment of cells resulted in a 0.88 fold decrease in TNF, while HuCD200-Fc displayed a 0.71 fold decrease in levels of secreted TNF. Results shown are from one representative animal of the four animals utilized. *** denotes an extremely significant difference compared with Fc treatment ($p < 0.001$).

Chapter 4

Summary and conclusions

1. Characterization of R15 transcripts during RRV infection

a. Classification of R15 transcripts

Chapter 2 of this dissertation describes the preliminary characterization of transcripts encoding R15 during RRV infection. Primary rhesus fibroblast cells were infected with RRV, and through common technique for assigning viral genes to a particular lytic gene class, transcripts encoding R15 were detected at 72 hours post-infection. Herpesvirus genes expressed at 72 hours post-infection, such as R15, are classified as late lytic genes. This classification differs from what has been reported for the homologous ORF in HHV-8, K14, which is detected at early time points during lytic infection. Similar to K14 transcripts, however, is the bi-cistronic nature of R15 transcripts with a viral GPCR encoding ORF, ORF74 (47, 116, 153, 209). Both R15 and K14 are the upstream ORFs of these bi-cistronic transcripts, suggesting that co-expression of these homologous ORFs with ORF74 is important for some aspect(s) of the viral life cycle for both RRV and HHV-8.

b. Unique splicing of R15 transcripts

Splicing of the homologous HHV-8 K14/ORF74 transcripts has been reported to take place, removing only the intergenic region of the transcript, while leaving both ORFs intact (116, 209). R15/ORF74 transcripts are also spliced, however, the coding

sequence for R15 is altered due to this splicing event. R15 encodes a vCD200 homologue, which is predicted to contain a transmembrane domain, and it is specifically this region that is removed during splicing of the transcript.

c. Protein expression from spliced transcripts

cDNA constructs corresponding to the unspliced and spliced R15-ORF74 regions of viral transcripts were generated to assess expression of epitope tagged vCD200 and vGPCR. Cells transfected with the cDNA construct corresponding to the unspliced R15-ORF74 transcript displayed vCD200 expression on the cell surface as detected by immunofluorescence and flow cytometry. Interestingly, cells expressing vCD200 from the cDNA construct corresponding to the spliced R15-ORF74 transcript lacked surface staining, while epitope-tagged vCD200 was detected in cell supernatants as revealed by Western blot analysis. From these expression data, it appears that during RRV infection, vCD200 is present in two forms, a membrane-bound form, and a secreted form. The production of a soluble vCD200 is a novel finding and has not been reported to occur in the case of HHV-8 K14 or cellular CD200.

Epitope tagged RRV vGPCR expression was also detected in cells transfected with both cDNA constructs as determined by immunofluorescence. However, Western blot analysis revealed that expression of epitope tagged vGPCR from the cDNA corresponding to the spliced transcript is reduced in comparison to protein levels from cells transfected with the unspliced cDNA construct. This R15-ORF74 splicing event removes the region upstream of the vGPCR start site, potentially

removing or altering a region important for translation initiation, such as a Kozak sequence, reducing the efficiency of translation. Translation of vGPCR that is occurring is likely through untraditional means, such as through an internal ribosomal entry site (IRES)-mediated mechanism, ribosomal scanning, or translation re-initiation. This report of vGPCR expression is the first to demonstrate vGPCR expression as the downstream ORF within a bi-cistronic message, as similar studies with HHV-8 ORF74 have not been performed.

2. Assessing function of RRV vCD200

a. Determining a suitable cell type for assessing RRV vCD200 function.

The function of RRV vCD200 is discussed in Chapter 3 of this dissertation. For these studies, a cell type expressing CD200R was required. While expression of CD200R has been detected on the surface of primary human macrophages and monocytes (230), CD200R expression on the surface of transformed cell lines has not been extensively determined. For example, the human monocytic cell line, U-937, is believed to lack CD200R expression, despite the myeloid lineage of these cells (77). The human monocytic cell line, THP-1, was first examined for levels of CD200R transcripts before and after differentiation with phorbol ester treatment. Transcripts encoding CD200R were present in monocytic THP-1 cells, and the levels of CD200R transcripts increased following differentiation. Next, CD200R protein expression was assessed on differentiated THP-1 cells. Immunofluorescence revealed CD200R

expression on the surface of differentiated THP-1 cells. THP-1 cells were therefore determined to be useful for examining the function of RRV vCD200.

b. RRV vCD200-Fc

A fusion protein was generated in which the predicted extracellular domain of vCD200 was fused with the Fc fragment of human IgG₁. When expressed in mammalian cells, vCD200-Fc was glycosylated, and due to the Fc component of vCD200-Fc, this protein dimerized. vCD200-Fc was also utilized as an antigen to generate a vCD200-specific monoclonal antibody that detected surface expression of vCD200 during RRV lytic infection of rhesus fibroblasts.

c. Myeloid cell treatment with vCD200-Fc

Incubation of myeloid cells with a functional CD200 homologue would result in a reduction in the production of type 1 cytokines, such as TNF. Activated human monocyte-derived macrophages treated with vCD200-Fc displayed reduced levels of transcripts encoding TNF and reduced levels of secreted TNF compared to controls. In addition to affecting human cells, vCD200-Fc treatment of primary rhesus macaque macrophages also resulted in reduced levels of secreted TNF. Taken together, RRV encodes a functional vCD200 homologue.

3. Role of vCD200 during RRV infection

a. Expression of R15 during RRV infection

While RRV and HHV-8 encode functional vCD200 homologues, the expression patterns of the respective ORFs differ during lytic infection. RRV R15 is expressed as a late lytic gene, while HHV-8 K14 expression occurs at an early time point following induction of latently infected cells into lytic viral replication (47, 116, 153). These differences in expression may actually exist, although another possibility that HHV-8 K14 expression may have been incorrectly characterized also exists. As our system of RRV infection of primary rhesus fibroblasts is strictly lytic, and each infection occurs *de novo*, classification of gene expression is straightforward. In the case of HHV-8, however, a model for *de novo* lytic infection does not currently exist, and researchers are limited to inducing latently infected cells to undergo lytic replication. HHV-8 lytic gene classification is further complicated in that a small percentage of latently infected cultures spontaneously enter lytic replication, so these transcripts may already exist before the cultures are induced to enter the lytic replication phase.

In addition to differing temporal expression, HHV-8 K14 and RRV R15 also differ in how they are expressed. HHV-8 K14 has been reported to express a classical membrane-bound vCD200 homologue (77), while splicing of transcripts containing RRV R15 results in the production of a membrane-bound and a secreted form (169). Considering that HHV-8 vCD200 is expressed early during lytic infection on the surface of infected cells, resident and infiltrating myeloid cells directly interacting with infected cells could be controlled in their activation, creating a cytokine environment conducive to the completion of HHV-8 lytic replication, thus allowing

for production of viral progeny. Expression of RRV vCD200 does not occur until late time points during lytic replication, therefore, this immune modulatory protein is limited simply by time in the potential effects it may have on myeloid cells directly interacting with infected cells, as the infected cell will soon lyse. Therefore, expression of a soluble form of RRV vCD200 could allow for the immune modulatory effects of RRV vCD200 to continue even in the absence of an intact infected cell membrane displaying RRV vCD200. Again, through controlling activation of nearby myeloid cells and thus the cytokine environment surrounding infected, secreted RRV vCD200 could enhance viral replication.

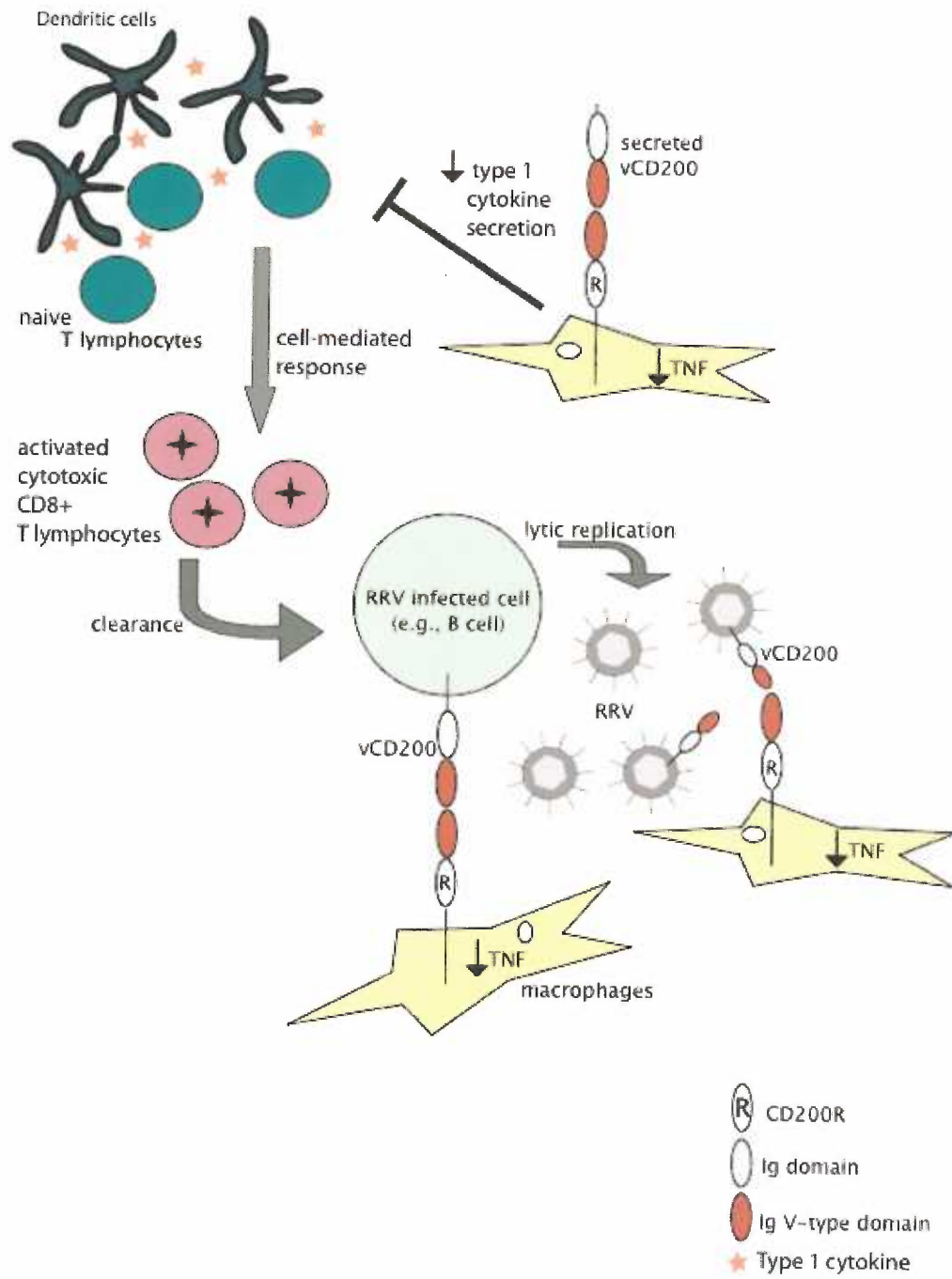
b. Model for RRV vCD200 action during infection

Expression of RRV vCD200 in two forms, a membrane-bound and a secreted form, creates the potential for delivery of immune modulatory effects on two levels. First, cytokine production from myeloid cells directly interacting with infected cells displaying RRV vCD200 will be controlled through binding of CD200R. Unique to RRV is the second mode of action, controlling cytokine secretion from myeloid cells infiltrating to the site of viral infection and not directly interacting with infected cells. In binding CD200R on cells of myeloid lineage, RRV vCD200 will effectively alter the function of the adaptive immune response. In the absence of vCD200 during RRV infection, macrophages responding to viral infection will secrete type 1 cytokines, including TNF. Within the draining lymph node, the type 1 cytokine environment during the priming event of naïve T cells by antigen presenting DCs will result in the production of T_H1 cells. T_H1 cells will then stimulate a cell-mediated immune

response, where CD8⁺ T cells become activated, and will eliminate virus-infected cells (refer to section 1.e). Instead, RRV vCD200/CD200R ligation on myeloid cells of the innate response (e.g., macrophages, monocytes) results in the reduction of type 1 cytokine secretion. A reduction in type 1 cytokines during naïve T cell priming, will result in a reduced cell-mediated anti-viral response, which will allow for successful replication, and establishment of RRV latency (Figure 4.1). Indeed, myxoma virus encoded vCD200 functions in controlling viral clearance by the host immune system as rabbits infected with myxoma virus lacking this molecule recovered from a normally fatal infection (33). Upon examination of T lymphocytes within infected animals, a greater number of activated CD8⁺ T lymphocytes were detected in those infected with myxoma lacking vCD200. In addition, reduced numbers of activated T lymphocytes were found in the lymph nodes of vCD200 knock-out virus infected animals compared to those infected with wild-type myxoma (33), strongly suggesting a defect in the priming and activation steps normally leading to the establishment of effective cell-mediated antiviral response.

In addition to controlling activation of CD200R⁺ cells, membrane-bound vCD200 may become incorporated into RRV virions as virions egress and bud through cellular membranes. Displaying vCD200 on the surface of virions may allow for entry into and subsequent infection of CD200R⁺ cells (Figure 4.1). CD200R⁺ cells, such as monocytes and macrophages, can serve as viral reservoirs, or they could be involved in dissemination of the virus throughout the host, increasing the probability for disease development.

Figure 4.1 Proposed model for RRV vCD200 action during RRV infection. As vCD200 is present as a membrane-bound and a soluble form, two routes of controlling the host immune response exist: controlling activation of CD200R⁺ cells by directly interacting with infected cells displaying vCD200 on their surface, and controlling activation of CD200R⁺ myeloid cells that have infiltrated to the site of infection through interacting with secreted vCD200. Both modes of immune modulation are induced through vCD200 binding to CD200R on cells of myeloid lineage (e.g., macrophages). In response to viral infection, without ligation of CD200R, macrophages become activated and secrete type 1 cytokines. The presence of type 1 cytokines during dendritic cell priming of naïve T lymphocytes leads to production of T_H1 T lymphocytes, which activate a cellular-mediated immune response executed by cytotoxic CD8⁺ T lymphocytes. The CD200R ligation by vCD200 reduces the secretion of type 1 cytokines from the macrophage, which will reduce the resulting cellular response to virus-infected cells. In addition to eliciting immune control, newly produced RRV virions could pick up vCD200 from cellular membranes through egress and budding, allowing the virion to bind and potentially gain access to CD200R⁺ cells.



4. Future directions

As RRV vCD200 is expressed as a secreted molecule in addition to the membrane-bound form, unique opportunities exist for utilization of this molecule in a transplant setting to increase allograft survival. As vCD200 has evolved with the rhesus macaque host and likely binds CD200R of rhesus macaque origin, the rhesus macaque is the ideal host for transplantation trials. To control lymphocyte secretion of type 1 cytokines often associated with graft rejection (181, 224), animals could be treated with soluble vCD200 prior to allograft transplant. Alternatively, donor specific dendritic cells expressing full-length or soluble vCD200 could be injected into the host prior to transplantation as these cells have proved useful in delivering tolerizing signals within murine transplant models (89).

5. Final conclusions

Utilizing RRV/SIV as the animal model of HIV/HHV-8 infection has proven to be promising, as the RRV ORFs that have been investigated to date have similar function to their counterparts in HHV-8 (57, 71, 109). RRV R15 is another of these ORFs sharing function with the homologue in HHV-8. Further understanding of the functions that viral ORFs play *in vitro* will continue to lend insight in the utility of the SIV/RRV infected rhesus macaque model for HIV/HHV-8 co-infected individuals. In addition, utilization of the RRV/SIV model will become increasingly advantageous over *in vitro* systems of HHV-8 infections as the RRV bacterial artificial chromosome

(BAC) technology becomes established. Using the BAC system, various knockout and HHV-8/RRV chimeric viruses can be generated, allowing for functional determinations of the contributions of individual viral ORFs to infection and disease development in rhesus macaques.

APPENDICIES

Appendix 1

Assessing RRV vFLIP anti-apoptotic activity

Introduction: In order for a virus to persist within a host, the host cell apoptotic response must be subverted. Rhesus rhadinovirus (RRV) encodes two proteins that are predicted to aid in blocking the host cell apoptotic response to viral infection: a vBcl-2 homologue encoded by ORF16 and a viral FLICE (FADD [Fas-associated death domain]-like IL-1 β -converting enzyme)-inhibitory protein (vFLIP) encoded by ORF71 (195). Based upon sequence homology with cellular counterparts, vBcl-2 likely blocks cell death mediated through mitochondria, whereas vFLIP is predicted to block signaling through the death receptor, CD95 (Fas/Apo-1). Expression of counterparts in HHV-8 suggests that RRV vBcl-2 is expressed during lytic infection (107, 205), and RRV vFLIP is expressed during latent infection (64, 107, 205), enhancing the survival of a virus infected cell at both stages of the viral infection. HHV-8 vFLIP activity has been confirmed (66) and will be utilized as a control for anti-apoptotic functions.

Ligation of trimerized death receptors (CD95) with natural ligand (FasL) or with activating antibody molecules induces death domain (DD) mediated interactions with the adapter protein, FADD. Next, inactive procaspase-8 binds to FADD through death effector domains (DED), resulting in self-cleavage and activation of caspase-8 (Figure A1.1A). This complex of proteins localized to activated CD95 is termed the death-inducing signaling complex (DISC), as activation of caspase-8 initiates the cascade of downstream caspase activation and eventual cell death (reviewed in (214)). Following caspase-8 activation, this cysteine protease cleaves and activates

caspase-3, which cleaves many cellular substrates including poly (ADP-ribose) (PARP), an enzyme involved in DNA repair (204). As PARP cleavage correlates with increased caspase activation, measuring the extent of PARP cleavage within an a cell can be used to determine the degree of cellular apoptosis (197, 215).

The structure of vFLIPs closely resembles that of the short form of cellular FLIP (FLIP_s), with each containing two DEDs that can interrupt the formation of the DISC at activated death receptors (Figure A1.1B). Specifically, vFLIPs, like FLIP_s, can bind procaspase-8 and/or FADD via DED interactions, blocking activation of caspase-8 (reviewed in (214)). We hypothesize that ligation of CD95 in the presence of RRV vFLIP will result in a decrease in activation of caspase-8 due to the interruption of DISC formation compared to cells not expressing RRV vFLIP. Concomitantly, we hypothesize that cells expressing vFLIP will contain lower levels of fragmented DNA and phosphatidylserine on the outer leaflet of the plasma membrane as well as lower levels of cleaved PARP than cells expressing empty vector, as a result of reduced caspase activation.

Materials and Methods: RRV ORF71 was amplified by PCR (Forward primer: 5'-AAGCTTGGGTCCATGTTCCCGCATAAG'-3', Reverse primer: 5'-ATCGATTTAACCGGGTGC GTT G-3') from RRV cosmid 28-2, and was subcloned into the expression vector pcDNA3.1(-) (Invitrogen Life Technologies) for expression in the murine B cells, A20 cells (American Type Culture Collection, Manassas, VA). A20 cells were electroporated (250 V, 975 μ F) with 5 μ g of DNA, and stable populations were selected for with G418 (Invitrogen Life Technologies) at 1.0